Clift *Progress in Earth and Planetary Science* (2017) 4:39
DOI 10.1186/s40645-017-0151-8

Progress in Earth and Planetary Science

REVIEW Open Access

Cenozoic sedimentary records of climate-tectonic coupling in the Western Himalaya

Peter D. Clift[1,2]

Abstract

Sedimentary archives in the Himalayan foreland basin and Indus submarine fan provide the most detailed records of how changing monsoon strength may have affected erosion and the development of tectonic structures in the western Himalaya during the Neogene. Muscovite Ar-Ar ages show that fast exhumation of the Greater Himalaya was earlier in the west (20–35 Ma) than in the central Himalaya (10–25 Ma), probably driven by progressive lithospheric slab tearing that caused both rock uplift and an intensified summer monsoon to start earlier in the western Himalaya. Rates of exhumation reduced after ~ 17 Ma as uplift also slowed, apparently unrelated to climate change. However, further reduction at 6–8 Ma coincided with a time of weakening summer rains, as shown by carbon isotope data from the foreland and hematite-goethite records from ODP Site 730 on the Oman margin. Coming at a time of stronger winds, this drying was linked to global climatic cooling. Weakening of Late Miocene monsoon rains coincided with a southward migration of the ITCZ and faster erosion of the Lesser rather than Greater Himalaya. Unroofing of the Inner Lesser Himalaya, starting after 9 Ma, followed as a consequence of duplex formation enabled by focused erosion, although widespread exposure of that range was delayed until after 6 Ma. Inner Lesser Himalayan exposure, combined with unroofing of the Nanga Parbat Massif, caused a decrease in average ε_{Nd} values of Indus River sediment after 5 Ma, rather than large-scale drainage capture.

Keywords: Monsoon, Climate-tectonic, Himalaya, Erosion, Exhumation, Arabian Sea, Foreland basin, Provenance, Geochemistry, Cenozoic, Weathering

Introduction

The building of high topography following the collision of India with Eurasia sometime in the early Cenozoic is proposed to have played a fundamental role in strengthening the Asian monsoon in South and East Asia (Kutzbach et al. 1993; Molnar et al. 1993). In turn, the monsoon climate is believed to feed back on the development of the mountains via surface processes and to partially control the tectonic evolution of the fold belts that have developed since the time of initial India-Eurasia collision (Clift et al. 2008; Whipple 2009; Willett 1999). In doing so, these interactions between the solid Earth and the atmosphere represent one of the world's great natural laboratories for studying the interplay of climate and tectonics over long periods of geological time. In particular, the Western Himalaya are a classic example of this interaction, despite being on the NW margin of the monsoon rainfall, which is centered instead around the Bay of Bengal. In fact, because of their location on the edge of the monsoon region, the Western Himalaya are more sensitive to changes in rainfall as monsoon precipitation waxed and waned. This area also has the advantage of having relatively well-documented, long-duration, marine paleoceanographic records (Prell et al. 1992; Kroon et al. 1991; Gupta et al. 2015), which can be compared readily with contemporaneous continental records.

In this review, I evaluate the evidence linking the climatic development of SW Asia to the processes of mountain building in the adjacent ranges of the Himalaya and Karakoram (Fig. 1), exploiting the sedimentary record preserved in the terrestrial and marine basins. This allows both the processes of erosion, as well as the environmental conditions that have affected the region since ~ 25 Ma to be compared. I focus on the Miocene to present, because this is the time period over which we have more complete records of terrestrial erosion and environmental conditions

Correspondence: pclift@lsu.edu
[1]Department of Geology and Geophysics, Louisiana State University, Baton Rouge, LA 70803, USA
[2]School of Geography Science, Nanjing Normal University, Nanjing 210023, China

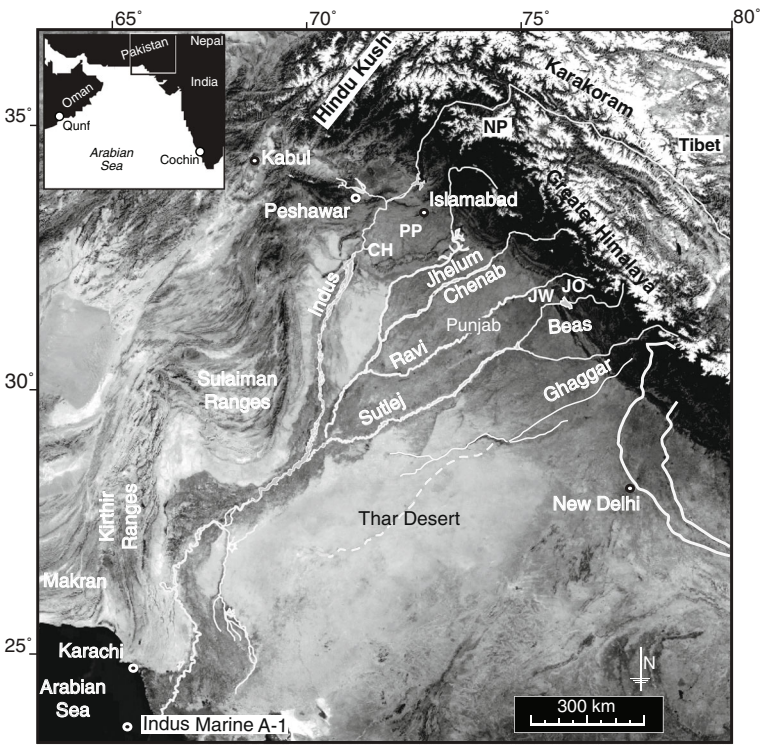

Fig. 1 Satellite image of the Indus Basin from Google Earth. Map shows the major tributaries and trunk stream of the Indus, together with the main ranges discussed in this study. PP—Potwar Plateau; CH—Chinji; NP—Nanga Parbat; JW—Jawalamukhi; JO—Jogindernagar

(Burbank et al. 1996; Najman 2006). It is also the time period for which new matching marine records are now available from scientific ocean drilling in the Arabian Sea (Pandey et al. 2015). Although climate-tectonic interactions may go back much further into the Paleogene, presently, there are no suitable sedimentary sequences in SW Asia that allow testing of whether the monsoon is really much older than the Miocene and whether the onset of mountain building immediately after India-Eurasia collision was linked to early Eocene intensification of summer rainfall, as has been proposed in some parts of South and East Asia (Licht et al. 2014).

The Indus River Basin

Much of the evidence constraining erosion and environmental conditions is preserved in the fill of the sedimentary basins of SW Asia, which have been supplied by the erosional load carried by the Indus River and its various tributaries (Fig. 1). This drainage system is the only major system in the western Himalaya (with the exception of the Oxus/Amu Darya flowing north from the Pamir) and comprises a trunk stream that originates in western Tibet that then flows westward along the Neotethyan Indus Suture Zone before turning south around the western syntaxis (Nanga Parbat) and heading to the Arabian Sea where it has supplied the material to construct the second largest sediment mass in the modern oceans, the Indus Submarine Fan (Fig. 2) (Clift et al. 2001; Naini and Kolla 1982; Kolla and Coumes 1987). The Indus Fan stretches >1500 km from the coast of Pakistan into the Indian Ocean and comprises ~4.5×10^6 km^3 of sediment, around a third of the size of the neighboring Bengal Fan.

On the eastern side of the drainage, the Indus River (average trunk discharge 3.91×10^6 m^3/s) (Alizai et al. 2011) is supplied by discharge from four large tributaries, the Jhellum (average discharge 9.9×10^5 m^3/s), Chenab (1.1×10^6 m^3/s), Ravi (2.6×10^5 m^3/s), and Sutlej (4.0×10^5 m^3/s) (Fig. 1) that largely derive their sediment from the Greater and Lesser Himalaya before flowing across the plains of the Punjab to join the mainstream about half way on its journey from the mountain front to the sea (Inam et al. 2007). In doing so, these rivers also fill the foreland basin that borders the Himalaya on their southern flank. A smaller set of flexural basins borders the Indus River to the west where the oblique collision between the Indian Plate and Eurasia, represented by the Chaman Fault, has generated SE-propagating thrust belts in the Kirthar and Sulaiman Ranges (Fig. 1) (Roddaz et al. 2011). There is little sediment supplied from the west into the Indus River because of the generally arid conditions. The major exception to

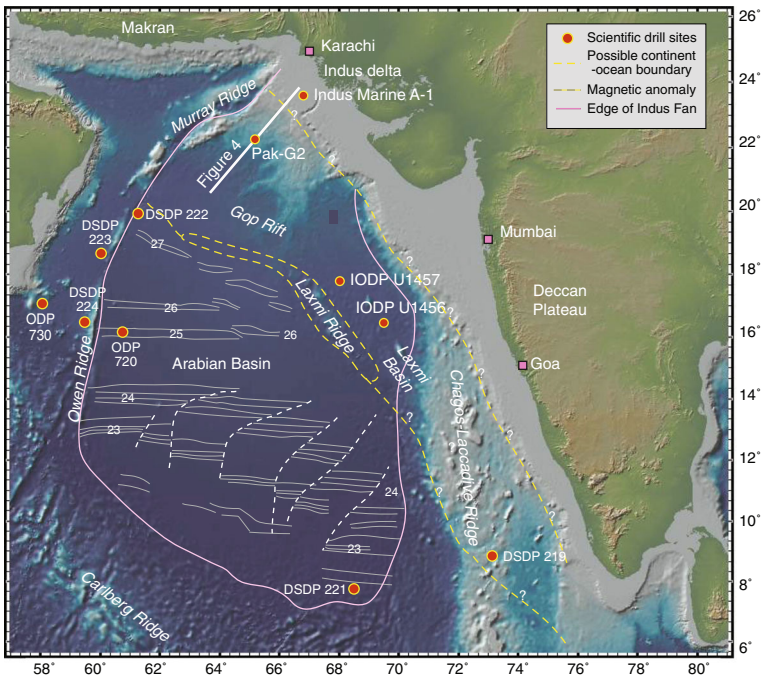

Fig. 2 Shaded bathymetric map of the Arabian Sea showing the extent of the Indus Fan (Kolla and Coumes 1987), the location of scientific and industrial boreholes discussed in this paper, and the main tectonic elements that bound the basin, especially the marine magnetic anomalies of Miles and Roest (1993). Base map is from GeoMapApp

this pattern is the Kabul River that brings sediment from the Hindu Kush.

Reconstructing erosion

If we are to assess the degree to which climate or solid Earth tectonic forces control the development of the Himalaya, then we need to derive independent records of how erosion and climate have evolved over long periods of geological time, in order to compare with the structural evolution of the mountains. This is most effectively done through detailed provenance studies that attempt to reconstruct how patterns and rates of erosion have changed through time, in order to determine whether changes in these processes correlate with climatic events. This is easier to do in the Indus River basin compared to many areas because of the compositional diversity of the source terranes. Figure 3 shows the different ranges and tectonic blocks that comprise the Western Himalaya and the associated ranges in the Karakoram and Hindu Kush. Each of these units has their own distinctive geological history and compositional characteristics that allow their influence on the net flux of sediment to the Arabian Sea to be resolved. Because of differences in the timing of tectonic or magmatic events in each block, the sediments eroded from each tends to have unique characteristics in terms of either geochemistry or the age of mineral cooling through a variety of different closure temperatures (Hodges 2003).

Source terrains

The Lesser, Greater, and Tethyan Himalaya comprise rock units that were previously part of a Greater India prior to its collision with Eurasia (Garzanti et al. 1987; Ali and Aitchison 2005). These units have some similarities in terms of their evolution prior to collision, although in general the rocks of the Lesser Himalaya tend to represent older crust (DeCelles et al. 2000; Gehrels et al. 2011), which has been more recently exhumed to the surface than the high mountains of the Greater Himalaya. Those in turn have been metamorphosed at higher temperatures and pressures compared to the lower ranges to the south (Searle 1996; Hodges and Silverberg 1988; Searle et al. 2006). The Tethyan Himalaya represent weakly metamorphosed sedimentary rocks whose origin was similar to the Greater Himalaya in representing the former sedimentary cover to the northern margin of Greater India (Robertson and Degnan 1994; Zhang et al. 2012; Garzanti 1993). To the north of these mountains lies the primitive mafic rocks of the Kohistan magmatic arc (Bignold et al. 2006; Khan et al. 1997), believed to have been formed in an intra-oceanic subduction setting, which is the primary geological unit within the Indus Suture Zone. In turn, the Kohistan Arc is juxtaposed along its northern edge

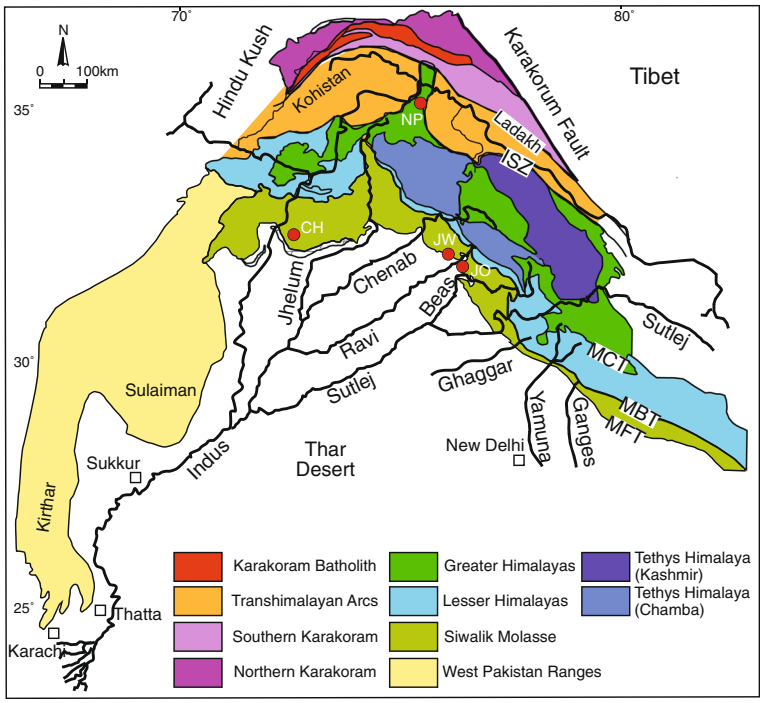

Fig. 3 Geological map of the study area showing the major tectonic units that are eroded by the Indus River and its tributaries. Map is modified after Garzanti et al. (2005). Rivers as shown in thick black lines. ISZ = Indus Suture Zone, MCT = Main Central Thrust, MBT = Main Boundary Thrust and MFT = Main Frontal Thrust. Sample locations are shown as filled circles. Thick black line shows major Himalayan tributaries. CH—Chinji; NP—Nanga Parbat; JW—Jawalamukhi; JO—Jogindernagar

against the Karakoram separated by the Shyok oceanic suture zone (Robertson and Collins 2002; Dunlap and Wysoczanski 2002). The Karakoram themselves represent a Mesozoic continental magmatic arc that preceded the closure of this northern Tethyan ocean but continued activity long after closure of the oceanic basin (Schärer et al. 1990; Searle et al. 1989; Fraser et al. 2001). Equivalent rocks in the Hindu Kush have similarities with the Karakoram but are generally not as strongly metamorphosed and have not experienced the recent high exhumation rates (Hildebrand et al. 2000), which are partly linked to activity along the Karakoram Fault starting in the middle Miocene (Phillips et al. 2004).

Another distinctive terrain within the Western Himalaya is the Nanga Parbat Massif that forms the linchpin of the Western Syntaxis (Fig. 1). This is well known as being a region of exceptionally fast rock uplift and exhumation, making it the source of young detritus into the Indus River (Zeitler et al. 1989; Treloar et al. 2000). However, earlier work on this system suggests that Nanga Parbat is less important as a source of sediment into the Indus than its Eastern equivalent at Namche Barwe (Lee et al. 2003; Clift et al. 2002b). In summary, the various ranges within the Indus basin have unique characteristics that allow their contribution to the erosional flux to be constrained if sufficient numbers of provenance proxies can be applied. Typically a single proxy is less effective at resolving erosional flux from a single tectonic block.

Marine sedimentary records

The vast majority (~ 66%) of the sediment eroded from the Himalaya since the Eocene lies in the Arabian Sea (Clift et al. 2001), even if some of the sediment was diverted to the west, into the Makran before the uplift of the Murray Ridge (Critelli et al. 1990). Although the region has been surveyed by seismic profiles over the thickest part of the depocenter, the bulk of the submarine fan has not yet been covered by representative seismic profiles. More importantly, the fan stratigraphy has not been penetrated to its total depth anywhere except the most distal locations in the southern part of the Arabian basin, for example at Deep Sea Drilling Project (DSDP) Site 221 (Whitmarsh et al. 1974). Most recently, International Ocean Discovery Program (IODP) recovered two sections from the Laxmi Basin, offshore Western India, IODP Sites U1456 and U1457 (Pandey et al. 2015). Although these provide relatively long records extending to ~ 10.8 Ma, they are unable to provide an erosional record of the Western

Himalaya back into the Paleogene. This is because of erosion of the fan in Laxmi Basin by the Nataraja Slide (mass transport deposit) that was deposited into the basin at around 10.8 Ma (Calvès et al. 2015). Furthermore, the IODP drill sites are unable to provide age control even to the younger part of the section across the proximal fan because they are separated from the main Arabian Basin by the Laxmi Ridge, preventing correlation of the dated reflectors from these sites towards the main sediment mass offshore the Indus River mouth.

Close to the modern river mouth around 11 km of sediment has been identified overlying igneous basement and carbonate sedimentary rocks (Clift et al. 2002a; Naini and Kolla 1982). The age of sedimentation here is only loosely controlled by industrial drilling sites both under the continental margin at Indus Marine A-1 (Shuaib and Tariq Shuaib 1999), as well as in deeper water at PAK-G2 (Fig. 4), which penetrated into Eocene carbonates related to the early stages breakup of the Arabian Sea. Although a detailed erosion budget is not possible at the present time, it is possible to date the onset of the construction of channel-levee complexes using the seismic and the industrial drilling data. This indicates that the first channel-levee complexes were being built during the Early Miocene and suggest a significant increase in sediment flux to the basin starting around that time (Clift et al. 2001; Droz and Bellaiche 1991). Nonetheless, several kilometers of sediment predate these features, indicating the longevity of the Indus River as the conveyor of sediment from the Western Himalaya since before the Early Miocene.

Sedimentology and mineralogy of the Himalayan foreland basin

To date most of the detailed reconstructions of erosion in the Western Himalaya have come from studies onshore, principally in the Himalayan foreland basin. As India has continued to move towards Eurasia, the plate has been flexed down by the weight of the subducting slab, as well as by the mountains resulting in a basin approximately 5–6 km deep (Raiverman et al. 1983). Sections of sediment from the basin have been progressively accreted into the mountains as the thrust front migrated southwards so that they are preserved both in the Sub-Himalaya and the Siwalik hills that form the first significant topography north of the Main Frontal Thrust (MFT). Figure 5 shows a generalized stratigraphic section of the sedimentary sequence. About half of the cumulative thickness is comprised of the Siwalik Group, which is a coarsening-upward sequence of fluvial rocks that date back to around 13 Ma (Burbank et al. 1996). These are principally dated through paleomagnetic methods coupled with radiometric dating of occasional volcanic ash beds that allow the depositional ages to be constrained (Ojha et al. 2000; Tauxe and Opdyke 1982; Johnson et al. 1985; Meigs et al. 1995). The Siwalik Group is divided into three different formations, with the Upper Siwalik being dominated by conglomerates of alluvial fan sedimentary facies (Rao 1993).

Although the coarsening-upward character might suggest an increasing intensity of erosion, this need not necessarily be the case because of the fact that any given point in a foreland basin will progressively approach the mountain front through time, as the Indian plate is underthrust, resulting in a long-term coarsening upwards even with constant erosional flux (DeCelles and

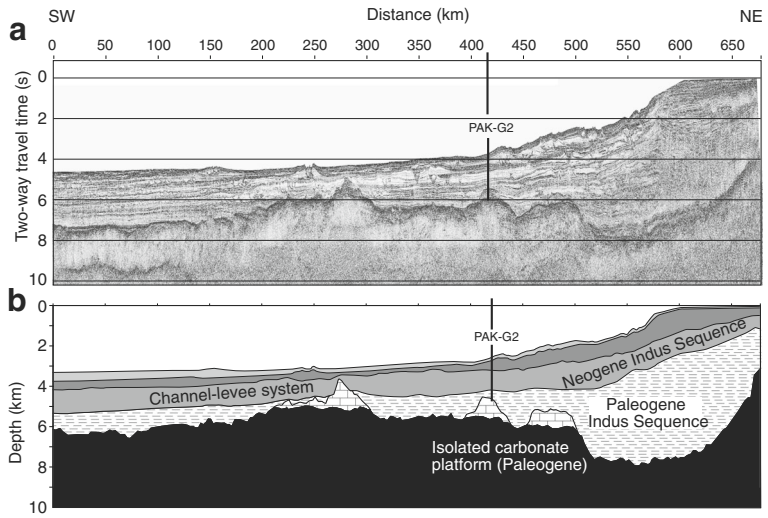

Fig. 4 NE-SW oriented seismic line TEPP207 through well PAK-G2, showing the original and interpreted sections. Modified from Calvès et al. (2008). See Fig. 2 for location

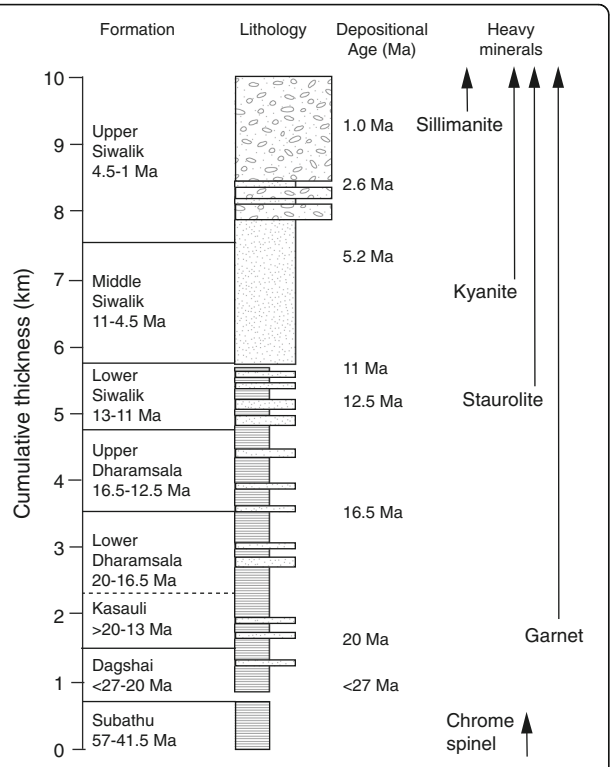

Fig. 5 Simplified stratigraphy of the western Himalayan foreland basin derived from the work of Jain et al. (2009), showing the general coarsening up-section and the appearance of a variety of higher grade metamorphic minerals that might be associated with the unroofing of the Greater and Inner Lesser Himalaya

Giles 1996). Those formations predating the Siwalik Group can be divided into two groups separated by a major unconformity of debatable duration but largely spanning the Oligocene. At one extreme, the hiatus spans from 40 to 22 Ma (Najman 2006; Jain et al. 2009), while others argue for a break of ≤ 3 m.y. or even less (Bera et al. 2008; Raiverman and Raman 1971). The muddy and carbonate rocks of the Subathu Formation at the base of the foreland section overlie older sedimentary rocks of the Indian Craton and have variously been interpreted as the products of sedimentation into an early foreland basin (Najman et al. 2001; Najman et al. 1997) or possibly into a back bulge location (i.e., on the distal side of the flexural forebulge) (DeCelles et al. 1998a). The Subathu sediments contain chrome spinel grains that were likely eroded from the Indus Suture Zone, presumably from ophiolites or magmatic units similar to those seen in Kohistan (Najman and Garzanti 2000). The units deposited above the long Oligocene (22–40 Ma) unconformity have a variety of names (Dagshai, Kasauli, Dharamsala, Murree and Kamlial Formations in the western foreland basin), but essentially comprise increasingly sandy fluvial sedimentary rcoks.

Studies of heavy minerals in these rocks show the appearance of garnet starting at about 20 Ma (Najman and Garzanti 2000; Sinha 1970), shortly after the onset of thrusting along the Main Central Thrust at ~ 24 Ma (Stephenson et al. 2001; Catlos et al. 2001), which is at least partly responsible for the exposure of the Greater Himalayan Sequence, one of the possible sources. It is however highly debatable whether the garnet grains in these sandstones were actually derived from these units because garnet is not unique to the Greater Himalaya. It is noteworthy that going up-section a series of increasingly high-grade metamorphic minerals were progressively input into the foreland basin. Staurolite appears in the Lower Siwalik Formation, after ~ 13 Ma (Fig. 5), while kyanite makes its initial appearance in the Upper Miocene, with sillimanite being the most recent addition within the Pleistocene Upper Siwalik Formation (Najman and Garzanti 2000). Sillimanite is formed at higher temperatures than kyanite, leading to the idea that this up-section evolution in detrital mineralogy reflects progressive unroofing of higher temperature source rocks. Quite what those sources might be is not immediately clear because the crystalline Inner Lesser Himalaya also comprise high-grade metamorphic rocks, similar in grade to some part of the Greater Himalaya (Célérier et al., 2009a, b). The presence of Miocene leucogranites in the Greater Himalaya does, however, provide a contrast to the generally lower temperature rocks of the sandwiching Lesser and Tethyan Himalaya (Searle and Fryer 1986; Vidal et al. 1982), and their erosion might provide a key indicator of Greater Himalayan erosion.

Isotopic constraints on evolving provenance

Contrasting crustal ages and petrogenesis has resulted in major differences in isotopic character between the different ranges of the Himalaya. In particular, Nd isotopes have been used to assess the origin of clastic sediments in the foreland basin and Indus Fan because of the large known compositional ranges in the sources and modern rivers (Clift et al. 2002b; Najman et al. 2009; Clift and Blusztajn 2005; Ahmad et al. 2000; Whittington et al. 1999). Furthermore, the Nd isotope ratio ($^{143}Nd/^{144}Nd$) of clastic sediment is not affected by transport or chemical weathering/diagenesis (Goldstein and Jacobsen 1988). Nd isotope composition in part reflects the average age of the crust being eroded. The data plotted in this study are provided in Table 1.

Here, I consider two isotope ratios ($^{143}Nd/^{144}Nd$) from the Himalayan foreland, one at Chinji in Pakistan (Chirouze et al. 2015), close to the location where the Indus River crosses the MFT, and another at Jawalamukhi which lies close to the Beas River (Fig. 1) (Najman et al. 2009). Each is expected to record the long-term evolution of these local river systems and thus the erosion of that part of the

Table 1 Synthesis of published Nd isotope data used in this study, together with a reference to the original sources from which they were derived

Sample	Age	$^{143}Nd/^{144}Nd$	± 2σ	Depositional Age (Ma)	εNd	Source
224-10R-1, 140 cm	Middle Eocene	0.512027	5	37.0	− 11.9	Clift and Blusztajn (2005)
224-10R-2, 49 cm	Middle Eocene	0.512357	5	37.5	− 5.5	Clift and Blusztajn (2005)
224-11R-2, 100 cm	Early Eocene	0.512159	5	50.0	− 9.3	Clift and Blusztajn (2005)
224-7R-1, 35 cm	Upper Oligocene	0.512071	5	26.5	− 11.1	Clift and Blusztajn (2005)
224-7R-CC, 0 cm	Upper Oligocene	0.512039	5	27.0	−11.7	Clift and Blusztajn (2005)
224-8R-2, 49 cm	Middle Oligocene	0.512049	5	28.0	− 11.5	Clift and Blusztajn (2005)
720A-3H-2, 110 cm	Pleistocene	0.511921	5	0.6	− 14.0	Clift and Blusztajn (2005)
720A-3H-2, 14 cm	Pleistocene	0.511996	5	0.6	− 12.5	Clift and Blusztajn (2005)
731A-40X-2, 103 cm	Lower Miocene	0.512051	5	20.0	− 11.5	Clift and Blusztajn (2005)
731C-13 W-1, 50 cm	Lower Oligocene	0.512066	5	29.0	− 11.2	Clift and Blusztajn (2005)
731C-19R-1, 50 cm	Lower Oligocene?	0.512037	9	31.0	− 11.7	Clift and Blusztajn (2005)
731C-1R-1, 50 cm	Lower Miocene	0.512003	5	16.0	− 12.4	Clift and Blusztajn (2005)
731C-21R-1, 50 cm	Middle Eocene (?)	0.512021	6	38.0	− 12.0	Clift and Blusztajn (2005)
731C-24R-1, 50 cm	Middle Eocene (?)	0.512001	10	40.0	− 12.4	Clift and Blusztajn (2005)
731C-2R-1, 50 cm	Lower Miocene	0.512071	5	21.5	− 11.1	Clift and Blusztajn (2005)
731C-7W-1, 50 cm	Upper Oligocene	0.512049	5	25.0	− 11.5	Clift and Blusztajn (2005)
IL3 0 – Chinji	Middle Miocene	0.512334	7	13.8	− 5.8	Chirouze et al. (2015)
IL4 – Chinji	Middle Miocene	0.512434	5	13.7	− 3.8	Chirouze et al. (2015)
IL5 – Chinji	Middle Miocene	0.512258	6	13.4	− 7.3	Chirouze et al. (2015)
IL6 – Chinji	Middle Miocene	0.512237	7	12.3	− 7.7	Chirouze et al. (2015)
IL7 – Chinji	Middle Miocene	0.512302	8	12.0	− 6.4	Chirouze et al. (2015)
IL7 – Chinji	Middle Miocene	0.512329	6	12.0	− 5.9	Chirouze et al. (2015)
IL8 – Chinji	Middle Miocene	0.512278	9	11.8	− 6.9	Chirouze et al. (2015)
IL9 – Chinji	Middle Miocene	0.512379	5	10.0	− 4.9	Chirouze et al. (2015)
Indus Marine A1, 1380 ft	Pliocene	0.512097	13	2.9	− 10.6	Clift and Blusztajn (2005)
Indus Marine A1, 1620 ft	Pliocene	0.512106	6	3.6	− 10.4	Clift and Blusztajn (2005)
Indus Marine A1, 2200 ft	Pliocene	0.512145	7	5.2	− 9.6	Clift and Blusztajn (2005)
Indus Marine A1, 3180 ft	Upper Miocene	0.512131	4	6.9	− 9.9	Clift and Blusztajn (2005)
Indus Marine A1, 4180 ft	Upper Miocene	0.512135	5	8.7	− 9.8	Clift and Blusztajn (2005)
Indus Marine A1, 4940 ft	Upper Miocene	0.512127	16	10.0	− 10.0	Clift and Blusztajn (2005)
Indus Marine A1, 5920 ft	Middle Miocene	0.512131	5	11.7	− 9.9	Clift and Blusztajn (2005)
Indus Marine A1, 6890 ft	Middle Miocene	0.512133	5	13.2	− 9.9	Clift and Blusztajn (2005)
Indus Marine A1, 7190 ft	Middle Miocene	0.512132	11	13.7	− 9.9	Clift and Blusztajn (2005)
Indus Marine A1, 7820 ft	Middle Miocene	0.512104	8	14.6	− 10.4	Clift and Blusztajn (2005)
Indus Marine A1, 8140 ft	Middle Miocene	0.512137	6	15.1	− 9.8	Clift and Blusztajn (2005)
Indus Marine A1, 8650 ft	Middle Miocene	0.512124	8	15.9	− 10.0	Clift and Blusztajn (2005)
Indus Marine A1, 9170 ft	Middle Miocene	0.512117	7	16.8	− 10.2	Clift and Blusztajn (2005)
JAM-Sr2	Late Paleocene	0.512273	9	57.5	− 7.0	Zhuang et al. (2015)
JW-03-1A-clast2	Jawalamukhi clast	0.511772	8	10.6	− 12.6	Najman et al. (2009)
JW-03-1A-clast3	Jawalamukhi clast	0.511762	8	10.6	− 12.3	Najman et al. (2009)
JW-03-1A-clast4	Jawalamukhi clast	0.511525	8	10.6	− 15.6	Najman et al. (2009)
JW-03-4A-clast1	Jawalamukhi clast	0.511847	10	10.9	− 10.6	Najman et al. (2009)
JW-03-4A-clast2	Jawalamukhi clast	0.512333	8	10.9	− 7.5	Najman et al. (2009)

Table 1 Synthesis of published Nd isotope data used in this study, together with a reference to the original sources from which they were derived *(Continued)*

Sample	Age	$^{143}Nd/^{144}Nd$	± 2σ	Depositional Age (Ma)	εNd	Source
JW03-3A	Jawalamukhi clast	0.511849	9	11.0	− 9.9	Najman et al. (2009)
JW03-3A	Jawalamukhi clast	0.511642	9	11.0	− 13.8	Najman et al. (2009)
JW03-3A	Jawalamukhi clast	0.511847	11	11.0	− 10.0	Najman et al. (2009)
JW03-3A-	Jawalamukhi clast	0.511801	9	11.0	− 10.5	Najman et al. (2009)
JW03-3B	Jawalamukhi clast	0.511864	7	11.3	− 8.4	Najman et al. (2009)
JW97-17B	Jawalamukhi clast	0.511570	8	8.8	− 15.0	Najman et al. (2009)
JW97-17B	Jawalamukhi clast	0.511309	9	8.8	− 20.0	Najman et al. (2009)
JW97-17B	Jawalamukhi clast	0.511857	5	8.8	− 10.3	Najman et al. (2009)
JW97-18B	Jawalamukhi clast	0.511331	5	8.3	− 19.5	Najman et al. (2009)
JW97-19A	Jawalamukhi mudstone	0.511735	8	4.5	− 17.6	Najman et al. (2009)
JW97-19B	Jawalamukhi clast	0.511391	5	5.2	− 19.1	Najman et al. (2009)
JW97-20B	Jawalamukhi clast	0.511303	6	5.6	− 19.8	Najman et al. (2009)
JW97-21B	Jawalamukhi mudstone	0.511647	8	5.5	− 19.3	Najman et al. (2009)
JW97-24B	Jawalamukhi mudstone	0.511881	9	9.5	− 14.8	Najman et al. (2009)
JW97-28A	Jawalamukhi mudstone	0.511956	9	8.5	− 13.3	Najman et al. (2009)
JW97-31A	Jawalamukhi mudstone	0.511875	8	10.5	− 14.9	Najman et al. (2009)
JW97-34C	Jawalamukhi clast	0.511331	9	7.7	− 19.5	Najman et al. (2009)
JW97-34C	Jawalamukhi clast	0.511300	13	7.7	− 20.0	Najman et al. (2009)
JW97-34C	Jawalamukhi clast	0.512273	9	7.7	− 2.8	Najman et al. (2009)
JW97-36B	Jawalamukhi clast	0.512088	9	7.3	− 7.8	Najman et al. (2009)
JW97-36B	Jawalamukhi clast	0.512192	11	7.3	− 7.7	Najman et al. (2009)
JW97-36B	Jawalamukhi clast	0.511873	11	7.3	− 9.2	Najman et al. (2009)
JW97-39B	Jawalamukhi mudstone	0.511897	11	6.5	− 14.5	Najman et al. (2009)
JW97-40A	Jawalamukhi mudstone	0.511909	5	11.5	− 14.2	Najman et al. (2009)
JW97-45B	Jawalamukhi mudstone	0.511861	7	12.5	− 15.2	Najman et al. (2009)
RKT-10-GC1	Early to Middle Paleocene	0.512622	7	61.6	− 0.2	Zhuang et al. (2015)
RKT-Sr1	Early Paleocene	0.512639	6	62.8	0.2	Zhuang et al. (2015)
SHN-Sr4	Early Eocene	0.512246	11	54.0	− 7.5	Zhuang et al. (2015)
SWN-Sr01	Early Paleocene	0.512648	6	64.9	0.4	Zhuang et al. (2015)
SWN-Sr04	Early Paleocene	0.512743	17	63.8	2.2	Zhuang et al. (2015)
SWN-Sr06	Campanian-Maastrichtian	0.512670	7	70.0	0.8	Zhuang et al. (2015)
SWN-Sr08	Middle Paleocene	0.512438	7	61.0	− 3.7	Zhuang et al. (2015)
SWN-Sr09	Middle Paleocene	0.512412	9	60.4	− 4.3	Zhuang et al. (2015)
SWN-Sr10	Middle Paleocene	0.512499	10	59.8	− 2.6	Zhuang et al. (2015)
SWN-Sr12	Middle Paleocene	0.512375	6	59.2	− 5.0	Zhuang et al. (2015)
SWN-Sr14	Early Miocene	0.511981	6	17.7	− 12.7	Zhuang et al. (2015)
SWN-Sr16	Early Miocene	0.511970	8	16.1	− 12.9	Zhuang et al. (2015)
SWN-Sr17	Late Early to Middle Miocene	0.512062	16	14.1	− 11.1	Zhuang et al. (2015)
SWN-Sr18	Late Early to Middle Miocene	0.512100	10	13.4	− 10.3	Zhuang et al. (2015)
SWN-Sr19	late early to middle Miocene	0.512009	11	12.5	− 12.1	Zhuang et al. (2015)
SWN-Sr20	Late early to middle Miocene	0.512096	5	11.6	− 10.4	Zhuang et al. (2015)
SWN-Sr21	Middle to Late Miocene	0.512137	9	8.4	− 9.6	Zhuang et al. (2015)
SWN-Sr22	Middle to Late Miocene	0.511961	7	6.9	− 13.1	Zhuang et al. (2015)

Table 1 Synthesis of published Nd isotope data used in this study, together with a reference to the original sources from which they were derived *(Continued)*

Sample	Age	$^{143}Nd/^{144}Nd$	± 2σ	Depositional Age (Ma)	εNd	Source
SWN-Sr23	Late Miocene	0.512151	8	5.3	− 9.3	Zhuang et al. (2015)
SWN-Sr24	Pliocene-Pleistocene	0.512016	13	2.7	− 12.0	Zhuang et al. (2015)
SWN-Sr26	Pliocene-Pleistocene	0.512011	8	0.5	− 12.1	Zhuang et al. (2015)
SWN-Sr27	Early Oligocene	0.511942	6	31.2	− 13.4	Zhuang et al. (2015)
SWN-Sr31	Early Miocene	0.511909	7	23.0	− 14.1	Zhuang et al. (2015)
SWN-Sr32	Early Miocene	0.511925	7	21.3	− 13.8	Zhuang et al. (2015)
SWN-Sr35	Early Miocene	0.512012	7	19.5	− 12.1	Zhuang et al. (2015)
SWN-Sr40	Late Early to Middle Miocene	0.512000	6	15.0	− 12.3	Zhuang et al. (2015)
SWN-Sr41	Middle to Late Miocene	0.512171	10	9.9	− 9.0	Zhuang et al. (2015)
SWN-Sr42	Early Paleocene	0.512670	6	66.0	0.8	Zhuang et al. (2015)

Himalaya upstream of that point. Paleomagnetic age constraints indicate that the Chinji section spans the period 8–17 Ma (Johnson et al. 1985), while the Jawalamukhi section captures the period 5–13 Ma (Meigs et al. 1995) (Fig. 6). As well as these proximal records, I consider Nd isotope records from the Kirthar and Sulaiman Ranges in the lower reaches of the Indus (Zhuang et al. 2015), as well as from offshore derived from samples from industrial well Indus Marine A-1 and a variety of Ocean Drilling Program (ODP) and Deep Sea Drilling Project (DSDP) sites on the Indus Fan and Murray Ridge (Clift and Blusztajn 2005).

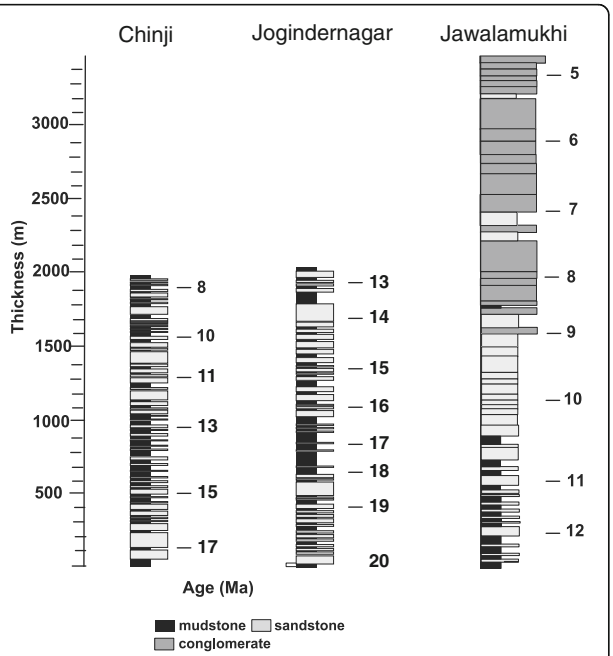

Fig. 6 Stratigraphic columns of three of the key foreland sections discussed in this paper, showing thickness, lithology and depositional ages. Chinji data are from Johnson et al. (1985), Jognidernagar data are from White et al. (2002), while Jawalamukhi data are from Najman et al. (2009). Note that the only well-studied section post-dating 8 Ma in the western Himalaya is at Jawalamukhi. None the sections extend older than 20 Ma meaning that they cannot be used to constrain changing erosion during the onset of rapid Greater Himalayan exhumation or the proposed intensification of the monsoon after ~ 24 Ma

Figure 7 shows how the Nd isotope ratio ($^{143}Nd/^{144}Nd$) of the clastic sediment has evolved through time since ~ 25 Ma. In this figure, I use the ε_{Nd} notation to describe the $^{143}Nd/^{144}Nd$ by normalizing these values to Chondrite Uniform Reservoir (CHUR) (DePaolo and Wasserburg 1976). The Kirthar Ranges and offshore data generally plot close to one another, as might be expected, and show a gradual increase from ε_{Nd} values of − 14 at 25 Ma to around − 9 by 10 Ma. Subsequently, ε_{Nd} values fell, especially after 5 Ma reaching values close to − 15 in the modern river (Clift and Blusztajn 2005). In general, higher ε_{Nd} values are associated with more erosion from the Karakoram and other rocks of the suture zone, with Himalayan erosion resulting in lower ε_{Nd} values. Thus, the records from the lower reaches of the paleo-Indus River system indicate increasing flux from the Karakoram before 10 Ma and then more Himalayan influence after that time.

Clift and Blusztajn (2005) interpreted the sharp change to lower ε_{Nd} values after 5 Ma to represent major drainage capture of the four Punjabi tributaries (Jhellum, Ravi, Chenab and Sutlje) into the Indus basin after that time, but more recent work at Chinji by Chirouze et al. (2015) now suggests that the change in ε_{Nd} values at the delta is probably linked to changes in the composition of the trunk river. The Chinji section sediments show ε_{Nd} values of around − 5 at 10–15 Ma, but the modern river close to Chinji has an ε_{Nd} value of − 11 (Fig. 7). This change was attributed by Chirouze et al. (2015) to reflect the start of erosion of the Nanga Parbat Massif after 5 Ma because Nanga Parbat is known to have very negative ε_{Nd} values (Whittington et al. 1999).

Nd isotope data from Jawalamukhi tells a different story concerning erosion of the Himalaya during the Neogene. As might be expected, given the location of

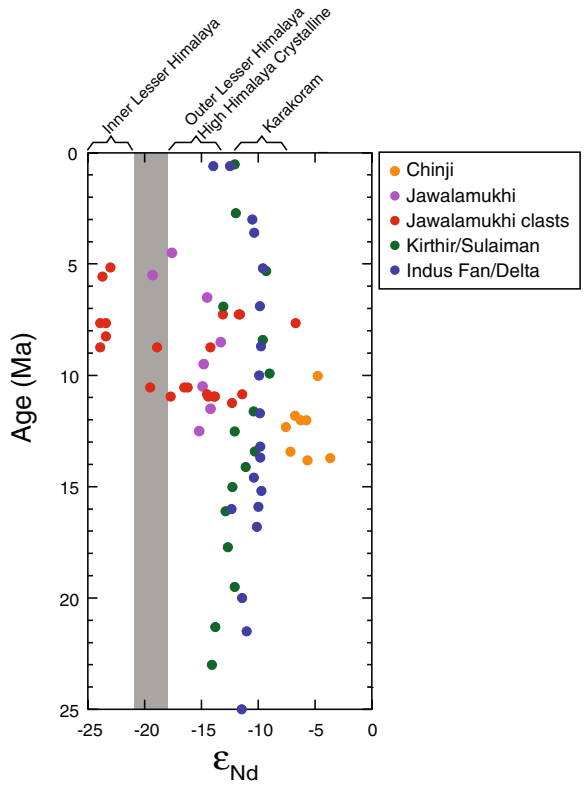

Fig. 7 Compilation of clastic sediment Nd isotope character from the Indus Basin since 25 Ma. Data from the Indus Shelf (Clift and Blusztajn 2005) and from the lower reaches in the Kirthir and Sulaiman Ranges (Zhuang et al. 2015) show a long term slow trend to more positive ε_{Nd} values followed by a drift to more negative ε_{Nd} values since ~ 5 Ma. In contrast, data from Chinji near the trunk Indus has consistently more positive ε_{Nd} reflecting the primitive sources in the suture zone (Chirouze et al. 2015). At Jawalamukhi in the eastern part of the drainage, ε_{Nd} values are more negative than the average. Extremely negative conglomerate clasts appear after ~ 9 Ma indicating erosion from the Inner Lesser Himalaya (Najman et al. 2009). Gray shading shows the demarcation between the Inner Lesser Himalaya and the Greater Himalayan Crystallines, Outer Lesser Himalaya and Karakoram

the section adjacent to Himalayan sources but far from the primitive sediment supply seen in the trunk river, ε_{Nd} values in those deposits are the most negative of any in the compiled dataset, reflective of their Himalayan sources (Najman et al. 2009). Prior to 9 Ma, both mudstones and conglomerate clasts in these sedimentary rocks show ε_{Nd} values close to − 15, consistent with erosion from the Greater Himalaya or from the Outer Lesser Himalaya. However, after 9 Ma conglomerate clasts with very negative ε_{Nd} values are found, falling to values close to − 25, which only readily correlate with the Inner Lesser Himalaya (Najman et al. 2009). As a result, Najman et al. (2009) concluded that the Inner Lesser Himalaya were only exposed at the surface after 9 Ma. Nonetheless, it is interesting to note that the isotopic composition of siltstones in the sequence continued to show ε_{Nd} values of around − 15, at least until around 6 Ma indicating that the total volume of material coming from the Inner Lesser Himalaya did not dominate over the Greater Himalayan material seen before that time. A shift to more negative ε_{Nd} values in the fine-grained sediment after around 6 Ma is however suggestive of an additional change starting at that time which can be further understood using thermochronologic evidence presented in the next section.

Thermochronology evidence for evolving erosion

Because the exhumation history of different source ranges changes across the Himalaya, the cooling ages of different minerals can be used to constrain where sediment sources. In particular, the application of Ar-Ar single grain muscovite mica dating has proven effective at resolving provenance within the foreland basin, as well as the Bengal Fan (Copeland and Harrison 1990). This is because the Greater Himalaya in NW India show rapid cooling starting in the Oligocene, largely ending in the Early Miocene (Stephenson et al. 2001; Walker et al. 1999), whereas the Inner Lesser Himalaya were not so deeply buried and were exposed to the surface more recently (Najman et al. 2009; Célérier et al., 2009a, b). Muscovite Ar-Ar ages are reset at temperatures at around 425 °C, consistent with burial in excess of around 15 km (Harrison et al. 2009). Because this is a relatively high temperature, these minerals are typically not reset during later burial in the foreland basin. Two sets of Ar-Ar detrital data have been collected from sections at Jawalamukhi (Najman et al. 2009) and Jogindernagar (White et al. 2002), which are relatively close to one another (Fig. 1) and which together provide a snapshot of erosion patterns and exhumation rates in that part of the Himalayan front since around 21 Ma.

Figure 8 shows the range of cooling ages for single mica grains compared with their depositional ages. A dashed line provides an indication of how rapid exhumation was by representing unity, i.e., when the two ages are within error of one another. Points plotting very close to this line are indicative of extremely rapid exhumation, such that grains can cool from 425 °C, and are then exhumed to the surface and deposited so quickly that the duration of grain erosion and transport is too short to be measured. The plot shows that at any given time there is typically a range of mica ages, some extending to significant ages of hundreds of m.y. or more. This pattern requires that both fast and slow cooling sources were contributing to the basin at any given particular time. It is, however, noteworthy that before around 17 Ma there is always a significant population of grains plotting very close to the unity line. This requires significant sediment flux from fast exhuming source areas. The fact that these Ar-Ar ages are

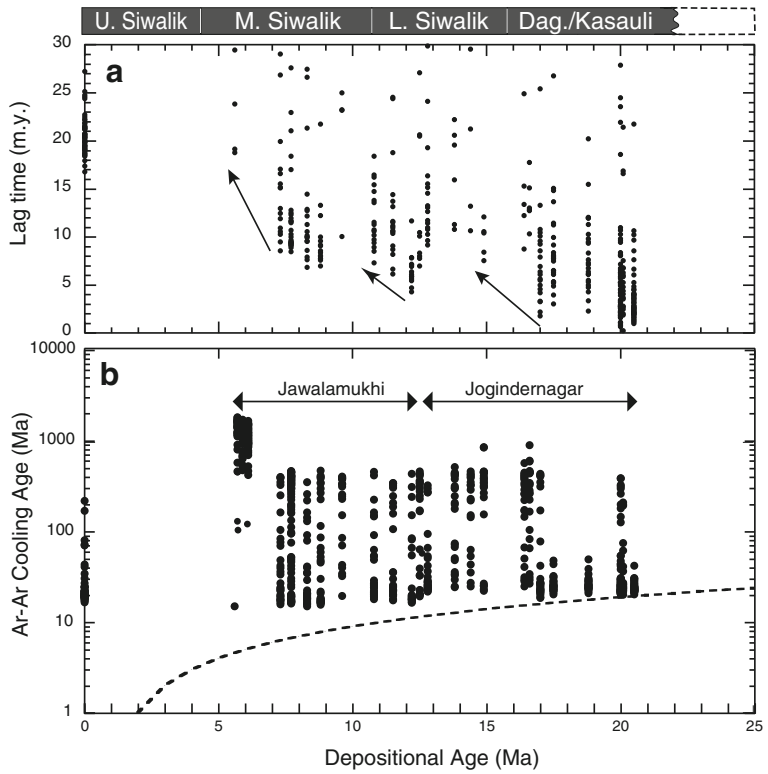

Fig. 8 Comparison of Ar-Ar muscovite cooling ages and depositional ages from the Jawalamukhi section of Najman et al. (2009) and the Jogindernagar section of White et al. (2002). Note that increase in lag of fastest cooled grains after ~ 17 Ma and ~ 8 Ma. **a** Lag times between cooling and sedimentation. **b** The cooling and deposition ages with the dashed line indicating zero lag time

Cenozoic indicates that those grains are derived from the Greater Himalaya or equivalent high-grade terranes exposed early on during the motion on the MCT. After 17 Ma, it is clear that there is a more discernable gap so that even the fastest cooled grains show a significant lag between cooling and deposition. Even though these young grains probably came from localized sources, this change was interpreted to indicate a slowing of exhumation rates in even these erosional "hotspots" after that time.

Figure 8a shows a close-up of the lag time of the fastest cooling grains for these data. This plot reinforces the conclusion that prior to 17 Ma at least some parts of the mountains were exhuming at very high rates but slowed after that time. It is also noteworthy that the lag time sharply increased after 6 Ma, with some more moderate slowing visible after 12 and 8 Ma as well. Najman et al. (2009) argued that a population with Paleozoic dates represented erosion from granites of that age, which have intruded the Crystalline Lesser Himalaya so that their appearance and dominance after 6 Ma were taken to indicate an exposure of that unit, at least in the watershed of these particular sections, corresponding now to the Beas River, close to Jawalamukhi. It is however unknown whether this change in erosion pattern and rate was a regional feature or related only to this particular area, as the section only preserves local rivers. Focused erosion along river valleys is well known to drive enhanced exhumation along these corridors (Montgomery and Stolar 2006; Simpson 2004), but this need not mean regional exposure of such units outside such restricted areas.

At a more regional scale, the examination of the Western Himalaya may be compared with other parts of the orogen by looking at the range of Ar-Ar cooling mica ages, as recently synthesized by Webb et al. (2017). Figure 9 shows the muscovite Ar-Ar ages seen across the entire foreland basin and which have been color-coded to show the longitude of sedimentation. This plot was designed so that the sediments at any one place might largely reflect the cooling history of the adjacent source ranges. What is clear is that the ages from the far western parts of the foreland basin have some of the oldest Ar-Ar ages of any sediment found in the Himalaya. They particularly contrast with those in the central Nepal Himalaya at around 83–86° East, which tend to cluster at ages of 15–20 Ma, compared to 25–35 Ma for muscovite Ar-Ar in northwest India (Fig. 9b). Such a distribution reveals a large-scale asymmetry where rapid cooling began earlier in the Indus Basin and later in the central Himalaya.

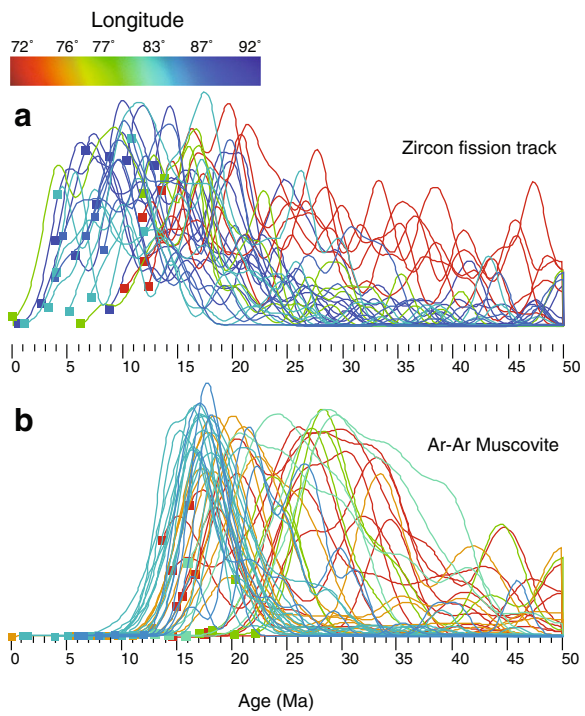

Fig. 9 Compilation of detrital thermochronology results from the Himalayan foreland basin, modified from Webb et al. (2017). Detrital thermochronology involves sampling sedimentary materials and acquiring cooling ages from detrital components, in order to constrain the cooling history of the sediment source regions. In parts **a** and **b**, $^{40}Ar/^{39}Ar$ muscovite and zircon fission track zircon results are plotted, respectively, for dates younger than 50 Ma. $^{40}Ar/^{39}Ar$ muscovite ages date the cooling of muscovite crystals below 425 ± 25 °C (Harrison et al. 2009), whereas fission track zircon ages date the cooling of zircon crystals below 240 ± 30 °C (Hurford 1986; Bernet and Garver 2005). The data are shown using the Kernel Density Estimation (KDE) methodology, which plots the detrital dates as a set of Gaussian distributions (Vermeesch 2012). This approach allows the age ranges and abundances of different detrital age populations to be compared: peaks in the curves represent peaks in the detrital age populations. For these plots, the population for a single sample is shown as a curve, sample longitude is keyed to a color spectrum, and the depositional age is shown via the squares at the young (left) terminations of the curve. These data provide an approximation of the cooling experienced by adjacent Himalayan regions. Signals in the Himalayan foreland basin can be complicated by river sediment transport along the range trend, since not all river systems transport sediment perpendicularly away from the mountains and thus might not only represent cooling and exhumation over the limited extent of the range immediately adjacent to the sampling location. A general trend appears in these data: peaks in the cooling age populations appear to young to the east from 25 to 20 Ma to 10–8 Ma. This is consistent with an eastwards migrating pulse of hinterland cooling and erosion during this period

The same general pattern was also shown in data from zircon fission track analysis (Fig. 9a), which dates the time at which detrital zircon grains cooled below around 200 °C (Hurford 1986; Tagami et al. 1990). Again, there are significant numbers of grains with old cooling ages extending back until 50 Ma, but ranging up until around 20 Ma in the Western foreland basin. In contrast, the central-eastern part of the foreland shows an onset to rapid cooling beginning in much younger times, generally after 20 Ma. Because these are detrital grains and not bedrock, we can be confident that this pattern is not a preservation issue linked to the removal of old material from the metamorphic rocks in the Greater Himalaya themselves but represents a real difference in the erosion history along the mountain chain. Because erosion tends to remove the older bedrock, the ages of the metamorphic and igneous rocks that now form the Greater Himalaya only tell us about the unroofing history of those particular rocks but do not help us constrain earlier erosion. This is only preserved in the sediments of the foreland basin or submarine fan.

The analysis by Webb et al. (2017) demonstrates that rapid cooling and erosion had began perhaps as early as the Late Eocene, and was certainly well underway during the Oligocene (30–35 Ma) within the Indus catchment. There was a period of rapid cooling around 20 Ma, shortly after the onset of motion on the MCT, with a corresponding drop off in rates shortly after that. As visible in Fig. 8a it seems that the basement sources began to cool more slowly after ~ 17 Ma. Webb et al. (2017) relate this burst of early cooling to a progressive breakoff of the subducting Indian lithospheric slab driven by a tear in the slab that propagated from the western syntaxis towards the east. This breakoff terminated crustal thickening and provoked a rebound of the Greater Himalaya that were then uplifted and incised rapidly, driving a wave of exhumation.

Changing rates of Himalayan erosion

Further detail about how erosion of the Western Himalaya differs from other parts of the range can be seen when considering studies from the central Himalaya. Bernet et al. (2006) conducted a study of the Siwalik Group in Western-Central Nepal where they applied zircon fission track dating to reconstruct the cooling history of that particular part of the Greater and Lesser Himalaya since 16 Ma. That study revealed that there were two groups of zircon fission track ages that remained essentially the same throughout the entire section and which pointed to relatively stable sources that continued to provide sediment to the basin at least since 16 Ma (Fig. 10). In contrast, after 11 Ma, a third minority age population appeared. This evolved to younger and younger ages as the sediment itself became younger. This implies the presence of a source that was rapidly uplifting and exhuming. Figure 10 demonstrates that this group had an approximate lag between cooling and sedimentation of 4 m.y. after 11 Ma. The younger of the stable fission track age populations centered around 16 Ma likely represents the Greater Himalaya (Bernet et al. 2006). The two younger sets of grains were interpreted to be derived from both the Greater and Lesser Himalaya, but

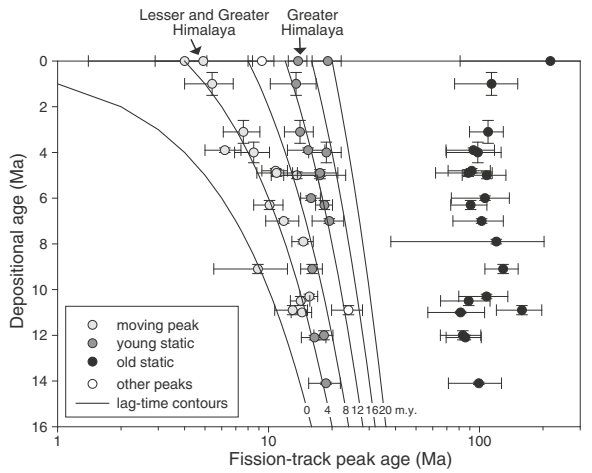

Fig. 10 Lag time plot of detrital zircon fission track peak ages versus depositional ages of Siwalik Group sedimentary rocks from Nepal and modern river sediment from Bernet et al. (2006). Peak ages are given with two σ errors. Old static peak refers to fission track age populations ~ 100 Ma and that do not change up-section. Young static peak refers to fission track age populations ~ 20 Ma and that do not change up-section. The young moving peak of fission track ages that appears after 11 Ma maintains a constant lag time of ~ 4 m.y. but constitutes a smaller fraction of the total sediment mass

particularly from the Lesser Himalaya, which became progressively more important as the Miocene progressed.

What is interesting to note in the study of Bernet et al. (2006) is that the rate of exhumation does not appear to speed or slow as time progressed towards the present day. This contrasts with the result from the muscovite Ar-Ar work at Jawalamukhi and Jogindernagar that implied a slowing of exhumation (Najman et al. 2009; White et al. 2002). Thus, either the micas and zircons were derived from different sources, or the exhumation history of the central Himalaya differs substantially from that seen in the Western Himalaya, potentially linked to the climatic gradient between them.

A note of caution is warranted however after considering what sort of record a slice of foreland strata might reflect. If those sediments were deposited close to the mountain front than they might reflect sediment being derived directly from the immediately adjacent ranges, whereas if the strata were deposited more centrally within the foreland they might show more evidence of material from a dominant axial river that is supplied by sediment from a broad region. This interplay between local and more regional influences was highlighted by Najman et al. (2009) in the case of the Jawalamukhi section where they inferred local dominance after 6 Ma due to the disappearance of flux from the Greater Himalaya. They reasonably presumed that the Greater Himalaya did not entirely stop eroding at that time and that the change in provenance in the preserved record was mostly linked to drainage reorganization at the local scale. Such local complexities are always an issue when dealing with proximal foreland sedimentary deposits. Although foreland sections will continue to be important, such complexity does highlight the additional need for a basin-wide view, such as provided by the integrated records from the Indian Ocean submarine fans.

Erosion and structural models of the Himalaya

Our understanding of how the Himalaya may have eroded based on the sedimentary records can now be compared with reconstructions concerning the orogenic architecture based on structural analysis. For example, Fig. 11 shows a reconstruction of the last 5.4 Ma derived from the work of Webb (2013). In this model, the Tethyan Himalaya essentially buried other structural units prior to 5.4 Ma and it is only after that time that they begin to come to the surface as a result of duplexing. The reconstruction at 1.9 Ma would appear to offer the first opportunity for rocks of the Greater Himalaya and of the Crystalline Lesser Himalaya to be exposed to the surface. This prediction would not necessarily preclude the changes in the rates of erosion demonstrated by the thermochronology data (e.g., Fig. 8). The structural reconstruction appears to indicate exposure of Inner Lesser Himalayan rocks a little later than would be inferred based on the Ar-Ar mica data from Najman et al. (2009) who showed the shift in provenance at about 6 Ma. However, the presence of conglomerate clasts from the Inner Lesser Himalaya seen at Jawalamukhi after 9 Ma would be much earlier than anticipated from the Webb (2013) structural model, but might reflect enhanced erosion along major river valleys (Simpson 2004; Montgomery and Stolar 2006) and reflect along-strike variability. It should be noted that other quite different structural and exhumation models have been proposed for the Himalayan foreland basin further east in Nepal. DeCelles et al. (1998b) used petrographic data from the pre-Siwalik Dumri Formation in Nepal to argue for erosion of sedimentary and low-grade metasedimentary rocks in the Tethyan Himalaya during the Early Miocene (~ 16–20 Ma). The presence of plagioclase grains in Dumri Formation sandstones suggested exposure of crystalline rocks of the Greater Himalaya at that time.

Certainly, the relative stability of Nd isotope composition until about 6 Ma in the siltstones of Jawalamukhi would also be consistent with relatively limited exposure of the Inner Lesser Himalaya until around that time. The Jawalamukhi isotope record is thus close to being in agreement with the structural reconstruction shown in Fig. 11. It is also noteworthy that the relatively late exposure of Inner Lesser Himalayan rocks predicted by the structural model would have served to input significant amounts of

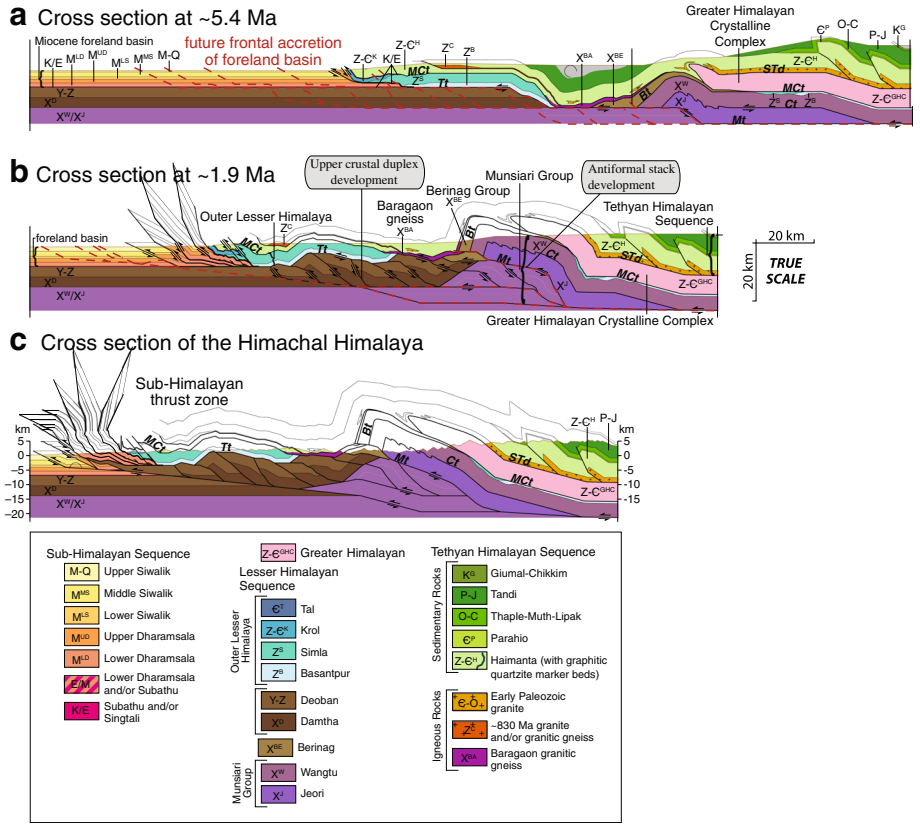

Fig. 11 Restorations of the Western Indian Himalaya by Webb (2013) at **a** ~5.4 Ma, **b** ~1.9 Ma and **c** the present day. Note that the crystalline Inner Lesser Himalaya and the Greater Himalaya are only predicted to breach the surface in this region after 5.4 Ma

relatively low ε_{Nd} material into the basin after 5.4 Ma. This provides an alternative mechanism to that suggested by Chirouze et al. (2015) to explain the basin-wide shift to more negative ε_{Nd} values after 5 Ma. Although the uplift and exposure of Nanga Parbat may have played a part in this process, it is possible that erosion of the volumetrically more important Lesser Himalaya were also driving the bulk Indus composition towards more negative ε_{Nd} values.

The Webb (2013) structural model is moreover consistent with the relatively recent appearance of both kyanite and sillimanite in the foreland basin as illustrated by Fig. 5, starting around 5 Ma at least in the Western Himalaya. Although the MCT must have been active much earlier, it appears that the final phase of erosion that brought kyanite and sillimanite-bearing sources to the surface may have been much more recent and not related either to motion along that fault, or to the slab break-off event that characterized the Oligocene to mid Miocene. Again, this may be linked to faster erosion caused by climatic variability. The apparent discrepancy between the Nepal reconstruction by DeCelles et al. (1998b) that requires earlier unroofing may indicate that one of these studies is in error or that there are major along strike differences in unroofing history. The much drier climate in the Indus basin might have slowed erosion and delayed Greater Himalayan unroofing compared to what is known in Nepal.

Erosion and climatic evolution

When trying to decide whether solid Earth tectonic forces or climate and surface processes control the structural evolution and exposure history of mountains, it is important to have an independent climate record to compare with erosional reconstruction in order to test for any linkages. There have been many attempts to try and reconstruct the evolution of the Asian monsoon over long periods of geological time, not all of which agree with one another. Kroon et al. (1991) looked at the varying abundance of *Globigerina bulloides*, a planktonic foraminifera that blooms offshore Oman during the summer monsoon because of the enhanced upwelling of nutrient-rich waters driven by the winds. These workers highlighted the time since 8 Ma as being one of intensified upwelling and therefore of stronger summer monsoon activity. Moreover, this reconstruction was broadly consistent with other evidence from the stable carbon isotope character of pedogenic carbonates within the Pakistani part of the foreland basin, i.e., the Potwar Plateau just to the east of Chinji. Quade et al. (1989)

showed a shift to more isotopically heavy carbon isotopes ($\delta^{13}C$) after ~7 Ma. This implied a shift from vegetation dominated by C_3 plant types, (i.e., mostly trees) to more C_4 domination (i.e., largely grassland). Although Quade et al. (1989) initially interpreted this to indicate a strengthening of the monsoon at that time, this was later changed to indicate a drying of the climate in the Indus floodplain after 7 Ma (Quade and Cerling 1995). The same general trend is also seen in NW India, where the first significant development of C_4 plants was dated at 7 Ma and with dominant C_4 growth after 5 Ma (Singh et al. 2011). The scatter to lower $\delta^{13}C$ values in NW India compared to Pakistan after 5 Ma may reflect the moderately wetter conditions seen going east along the Himalayan front and which favor C_3 flora (Fig. 12b). Oxygen isotopes have helped to confirm this interpretation of the vegetation changes. Dettman et al. (2001) provided oxygen isotope profiles through fossil freshwater bivalve shells and mammal teeth that help to constrain total rainfall and seasonality through the Late Miocene. These data showed the presence of a monsoon since at least 10.7 Ma but also demonstrated that the

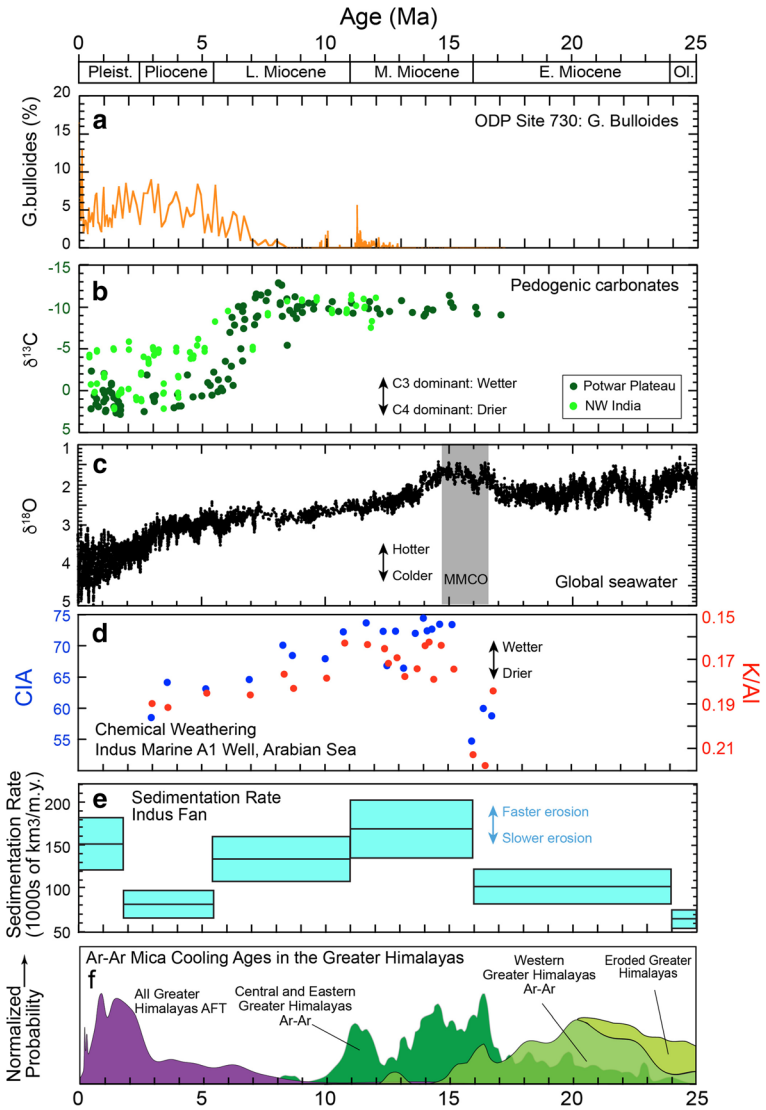

Fig. 12 Comparison of climate, erosion and exhumation proxies in the Himalaya. **a** Abundance of *G. bulloides* at ODP Site 730 on the Oman margin as a proxy for summer monsoon wind strength (Gupta et al. 2015). **b** Carbon isotope character of pedogenic carbonate in Pakistan as an indicator of dominant vegetation in the Potwar Plateau of Pakistan (Quade et al. 1989), and NW India (Singh et al. 2011). **c** Global d18O as a proxy for seawater temperatures and/or ice volume from Zachos et al. (2001). **d** Degree of chemical alteration of sediments on the Indus continental shelf at Indus Marine A-1 as measured by K/Al and CIA (Clift et al. 2008), **e** Rates of sediment supply to the Arabian Sea calculated from regional seismic (Clift 2006). **f** Exhumation rates of the Greater Himalaya tracked by bedrock Ar-Ar dating (Clift et al. 2008) and foreland basin sediment (Szulc et al. 2006)

$\delta^{18}O$ of wet-season rainfall was significantly more negative before 7.5 Ma than after that time. Assuming that there was not a big change in source water compositions at that time this shift in $\delta^{18}O$ would imply increasing aridity after 7.5 Ma.

Such interpretations beg the question as to why the climate would dry at a time when summer monsoon driven upwelling in the Indian Ocean appeared to be intensifying. It should be remembered that the upwelling proxy does not record summer rain, but rather is linked to the wind strength, which might potentially be decoupled from one another in the context of long-term global cooling during the Late Miocene. This is despite the fact that in the present day, coastal upwelling is largely modulated by summer monsoon winds that are also linked to precipitation in SW Asia (Curry et al. 1992). Chemical weathering records from the Indus continental margin show long-term decrease in the degree of alteration especially after around 10 Ma (Clift et al. 2008) that might indicate weaker monsoon over that timescale (Fig. 12d). Because humidity as well as temperature is a key control over the rates of chemical weathering (West et al. 2005), Clift et al. (2008) argued that the decrease in the degree of alteration seen in Indus River delta sediments reflects a drying of the climate after 10 Ma, broadly consistent with the carbon isotope data from the foreland basin. However, reconstructions from the South China Sea now suggest that falling global temperatures are the primary control on weathering rates, at least in southern China (Wan et al. 2012; Clift et al. 2014).

Although the age of drying/cooling inferred from weathering records appears to precede the 8 Ma upwelling increase documented by Kroon et al. (1991), it should be noted that more recent attempts to look at the abundance of *G. bulloides* have resulted in a reevaluation of the record. Although upwelling strengthened after 8 Ma, it is noteworthy that the initial increase began around 13 Ma (Gupta et al. 2015) (Fig. 12a). This older age for intensified wind strength is consistent with new results from scientific ocean drilling in the Maldives that showed the development of a large sediment drift link to prevailing monsoon winds, again starting at around 12.9 Ma (Betzler et al. 2016).

A new record for environmental evolution during this critical transition around 8 Ma is presented here based on new spectral color data scanned from ODP Site 730, the same site analyzed for *G. bulloides*. This analysis is based on the recognition that hematite and goethite are associated with characteristic wavelengths in the spectrum of the sediment (Deaton and Balsam 1991; Balsam and Deaton 1991). The ratio of these two wavelengths can be used to estimate the relative intensity of these two minerals (Giosan et al. 2002). This is significant because hematite is generally associated with hotter, drier, and more seasonal conditions, whereas goethite is more commonly recognized as a proxy for wetter, colder environments (Schwertmann 1971). Such an approach has been used effectively before in the South China Sea (Zhang et al. 2007; Clift 2006) as a means for tracking continental humidity and thus monsoon strength.

Figure 13 shows the hematite/goethite record from 10.7 to 8.5 Ma. Given the location of the core, this is presumed to reflect environmental conditions in Eastern Arabia, which is the source of the clastic sediment deposited at this drill site. Although there is a period between 9.9 and 9.5 Ma when hematite is relatively scarce, the overall trend after 9.5 Ma is towards more hematite-rich, presumably drier, more seasonal conditions. Such a record is consistent with the other proxies for chemical weathering and sediment supply that favors reducing precipitation and colder conditions, linked to a weakening summer monsoon into the Late Miocene. Exactly why the summer monsoon might be weakening at that time is not entirely clear, but could be related to the overall cooling of global climate at that time (Zachos et al. 2001), since times of cool dry conditions globally tend to correlate with times of weaker summer monsoons (Gupta et al. 2003; Clemens et al. 2010).

Although there has been some debate in the past concerning whether wetter climates might result in more or less erosion (Burbank et al. 1993), studies of the Quaternary evolution of the Indus and Ganges deltas have shown that sediment supply increased during times of strong monsoon (Clift and Giosan 2014; Goodbred and Kuehl 2000) when landsliding is also known to be common in the source areas (Bookhagen et al. 2005). This particular form of mountain erosion is well recognized as being particularly efficient at generating large volumes of sediment (Liu and Li 2015; Hovius and Stark 2006). It is thus interesting to note that the supply of sediment to the Indus delta and fan was estimated to peak during the middle Miocene, based on the interpretation of regional seismic reflection data coupled with sediment decompaction calculations (Fig. 12e) (Clift 2006). That reconstruction suggested that sediment delivery rates to the Arabian Sea dropped after the Middle Miocene to reach a minimum in the Pliocene, before rebounding to higher values during the Pleistocene. High rates of sediment delivery during the Middle Miocene coincided with times of stronger chemical weathering and suggest wet, more erosive climatic conditions at that time, at least in the Western Himalaya. Falling rates of sediment delivery and reduced erosion would then correlate with the drying climate in the Late Miocene, consistent with the pedogenic carbonate stable isotope data.

When considering the entire Himalayan range times of strong precipitation and rapid erosion broadly

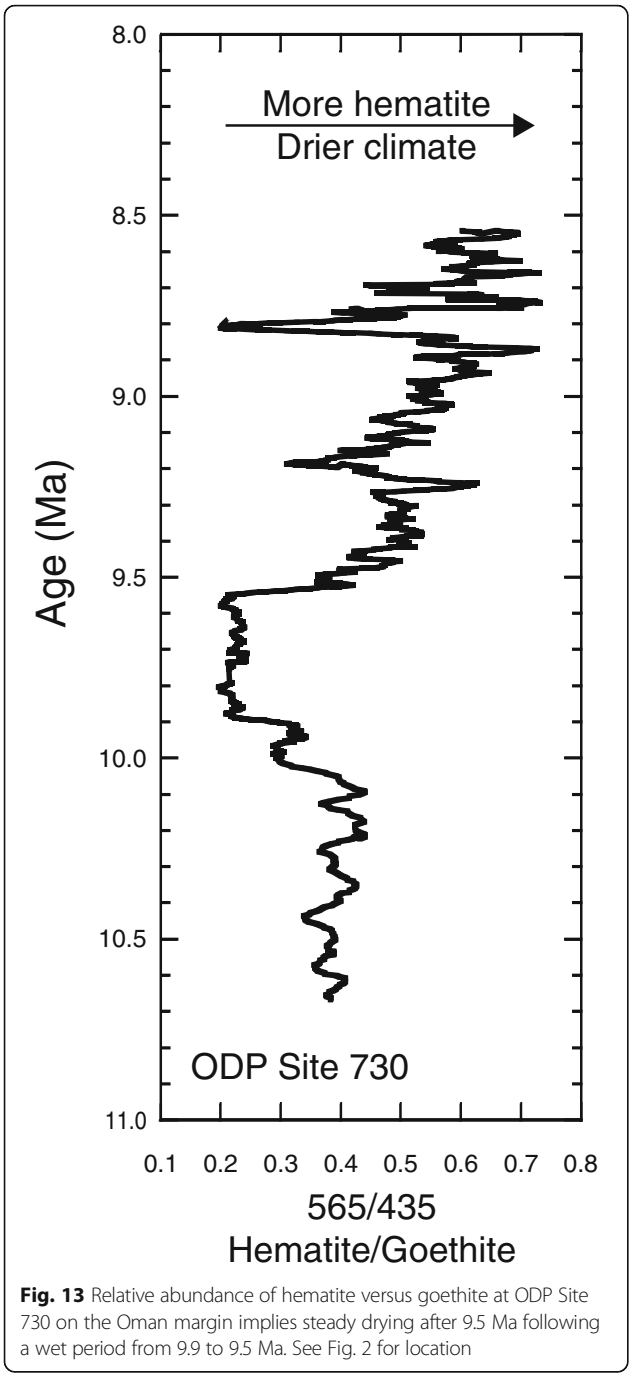

Fig. 13 Relative abundance of hematite versus goethite at ODP Site 730 on the Oman margin implies steady drying after 9.5 Ma following a wet period from 9.9 to 9.5 Ma. See Fig. 2 for location

correlate with episodes of fastest exhumation in the central and in Eastern Himalaya (Clift et al. 2008), but it is noteworthy that the time of fastest exhumation is oldest in the West (Webb et al. 2017). It is possible that this earlier phase of erosion relates to the initial phases of monsoon intensification whose timing is not well defined but appears to strengthen around 23 Ma based on data from the South China Sea (Clift et al. 2008). Unfortunately, no matching record from that time yet exists in the Arabian Sea. Certainly, detrital thermochronology from the foreland basin indicate that rapid erosion of the Western Greater Himalaya had begun during the Oligocene (Fig. 9) and that this would be consistent with an earlier initiation of the South Asian monsoon, as well as potentially with slab break-off (Webb et al. 2017).

Given that the climate is drier in the Western Himalaya compared to the eastern and central ranges, slower erosion in that former area would result in older fission track cooling ages being preserved in the bedrock sources. In contrast, faster erosion under the wetter climate in the East has stripped away bedrock with the older ages, which are only preserved in the Greater Himalayan crystallines exposed in the west. Alternatively, if the slab breakoff mechanism proposed by Webb et al. (2017) is correct, then the difference in fission track cooling ages may simply reflect the propagation of the tear and uplift from west to east during the Miocene.

Climate-tectonic linkages

Because the intensity of the South Asian monsoon has been modeled to be largely dependent on the height of the Himalayan barrier (Boos and Kuang 2010) rather than on the height and extent of the Tibetan Plateau, as previously favored (Kutzbach et al. 1993; Molnar et al. 1993), rebound of the Greater Himalaya caused by slab breakoff would have raised the topographic barrier along the southern edge of the Tibetan Plateau and driven a progressive increase in South Asian monsoon intensity starting shortly after ~ 30 Ma. Evidence for tearing of the Indian slab comes from a variety of sources. Seismic tomographic images of the mantle below India show a seismically fast region interpreted as detached Indian lithosphere (Replumaz et al. 2010). The distance between the detached slab and the Indian plate now underthrusting the plateau reduces from west to east leading Replumaz et al. (2010) to propose a lateral migration of slab detachment from the western Himalaya to the central Himalaya. These authors further estimated this tearing to have occurred from 25 to 15 Ma. This seismic evidence is further supported by an east-to-west younging of alkaline and adakitic magmatic rocks that are dated at ~ 17–19 Ma at the western end of the Himalaya, 25–30 Ma in the East and ~ 15–8 Ma in the east-central Himalaya has been interpreted as a product of lateral migration of slab detachment (Zhang et al. 2014; Pan et al. 2012).

In this scenario, the earlier onset of rapid erosion in the Western Greater Himalaya would be linked not only to uplift of the range caused by slab breakoff, but by a synchronous intensification of summer monsoon rains in that region driven by the increased height of the topographic barrier (Webb et al. 2017). Evidence for the height of the barrier is however rather thin. Hydrogen

isotope data from minerals in shear zones around Mount Everest indicating that the barrier in that location was > 5 km in the late Early Miocene (Gébelin et al. 2013), but no similar dataset is known from those mountains in the Indus catchment. Likewise, stable oxygen isotope data, which is sensitive to paleo-altitudes, from Miocene-Pliocene carbonate sediments in southern Nepal has been used to demonstrate altitudes of the southern Tibetan Plateau close to the present data before 11 Ma (Garzione et al. 2000). Similar data would argue for altitudes > 4 km in the central Tibetan Plateau as long ago as 35 Ma (Rowley and Currie 2006). Not only do these data not constrain elevations in the western Himalaya but also they largely relate to the plateau and not the Himalayan barrier.

Unfortunately, a sedimentary record of environmental conditions and erosion during the Oligocene is mostly not present in the Himalayan foreland basin because of the long-duration unconformity that separates the Subathu Formation from the Dagshai Formation (Najman 2006). Although it has been suggested that this gap reflects a forebulge unconformity (DeCelles et al. 1998a), more recently, it has been suggested that this hiatus is instead the product of rebound of the foreland basin caused by faster erosion in the mountains, which reduced the size of the orogenic load, thus allowing the foreland basin to partially invert during the Early Miocene (Clift and VanLaningham 2010). A similar erosion-driven inversion has been proposed from the Himalayas during the recent glacial episodes (Burbank 1992). In this model the great foreland unconformity is another reflection, together with the rapid exhumation of the Greater Himalaya, of an intensifying summer monsoon. However, if the slab breakoff model is valid, then this might also result in a flexural uplift of the foreland basin and the generation of a regional unconformity as the tear propagated from West into the central Himalaya. It is possible that both mechanisms may be playing a role in the development of this break in the record. Either way, the only sedimentary record that spans this critical period must be in the Arabian Sea and this has yet to be recovered by scientific ocean drilling. Until this is remedied, it is unknown when South Asian climate first became strongly monsoonal and if that is linked to faster erosion.

Given the incompleteness of the record, is it possible to say anything meaningful about the role of solid Earth tectonic processes compared to climatically modulated surface processes in controlling the erosion of the Western Himalaya? Slowing of erosion after around 17 Ma does not obviously correlate with any known climatic transition although it does shortly follow the warmest conditions of the Mid-Miocene Climatic Optimum (MMCO), which is expected to be a period of strong tropical rainfall (You et al. 2009; Wan et al. 2009). Instead, slowing exhumation after the Mid Miocene may reflect slowing uplift related to earlier slab breakoff, which triggered the initial phase of rapid exhumation seen to peak in the Western Himalaya at 24–17 Ma (Figs. 8b and 12). The Ar-Ar mica data points to a slowing of exhumation after around 12 Ma (Fig. 8b), which correlates well to the strengthening wind conditions in the Arabian Sea (Betzler et al. 2016; Gupta et al. 2015) (Fig. 12a). It is possible that the Late Miocene slowing of erosion might be related to an initial weakening of summer monsoon rain linked to global cooling that occurs at and just before that time (Zachos et al. 2001) (Fig. 12c).

A more straightforward link to climatic conditions can be seen in the slowing of exhumation rates after ~ 7 Ma. This is the time when the Ar-Ar data indicate reduced cooling rates and is when environmental conditions in the Indus floodplain became drier (Quade and Cerling 1995), with lower degrees of chemical weathering and reduced sediment flux to the ocean (Clift et al. 2008). What is less clear is why reduced erosion rates and a weaker monsoon would result in the exhumation of the Inner Lesser Himalaya. This may be the simple culmination of a long-term process by which these rocks are being progressively unroofed through time. Although the monsoon is weaker in the Late Miocene than during the Middle Miocene, it was still active and would have eventually exposed Lesser Himalayan units as a result of the rock uplift driven by the structural imbrication then occurring at depth. This view implies that exposure would have been largely driven by solid Earth tectonic processes. Alternatively weakening monsoon might have resulted in a southward migration of the band of most intense rainfall (i.e., the Intertropical Convergence Zone; ITCZ), which would have been pushed further north onto the edge at the Tibetan Plateau during times of strong summer monsoon. A review by Armstrong and Allen (2011) has proposed that the ITCZ has migrate southward during the Neogene. This model was largely based on the position of the smectite–illite transition that marks the boundary between wind-blown clay derived from Asia and that from Central and South America in the central Pacific Ocean (Lyle et al. 2002). In the western Pacific, a less dramatic migration southward was noted on the basis of the composition of manganese crusts that are dependent on biologic and detrital fluxes (Kim et al. 2006). As the monsoon weakened, this band of intense rainfall would have migrated south and became positioned over the region where the Inner Lesser Himalaya are now exposed. Analog modeling of the formation of duplexes in mountain belts suggests that these are preferentially formed beneath areas where surface processes are driving intensified erosion (Malavieille 2010). Formation of a duplex in the Inner

Lesser Himalaya after 5.4 Ma is indicative of intensified erosion in this region, linked to migration of the climatic bands associated with the summer monsoon.

The weakening of the summer monsoon during the Late Miocene does however appear to be largely linked to global cooling and not to changes in the height of the Himalayan topographic barrier, which was inferred to control monsoon strength during the initial intensification during the later Oligocene to early Miocene (Webb et al. 2017). In that model, exhumation of the Lesser Himalaya is largely driven by changes in summer monsoon intensity and location rather than solid Earth processes, which tended to be more steady state. The Late Miocene to Pliocene exposure of the Lesser Himalaya and duplex formation can be linked to monsoon evolution driven by global climatic processes.

Conclusions

Sedimentary records from the Himalayan foreland and Arabian Sea show that changing environmental conditions linked to summer monsoon intensity played an important role in controlling the structural evolution of the Himalaya. Greater Himalaya exhumation started earlier in the western than the central Himalaya, possibly linked to lithospheric slab breakoff that drove rock uplift and intensified the summer monsoon by raising the topographic barrier of the Himalaya. This in turn further increased erosion rates that peaked in the Middle Miocene in the Indus Fan. A regional unconformity in the foreland basin in the Oligocene to Early Miocene reflects both uplift driven by slab breakoff and the strengthening monsoon that heightened erosion rates and reduced the orogenic load on the subducting plate. However, the presence of the unconformity means that deep sea records are required if we are to extend our reconstruction beyond 20 Ma and so better correlate climate and erosion with Greater Himalayan exhumation.

Ar-Ar ages from detrital micas in the foreland basin indicate that exhumation in the NW Himalaya slowed after 17 Ma, apparently unrelated to monsoon variability. Initial strengthening of monsoonal winds is now dated to start at 12.9 Ma but is not positively correlated with South Asian rainfall. Indeed, exhumation rates appear to slow after 12 Ma implying a drier, less erosive climate. Stronger drying of the climate is documented after ~ 10 Ma, as shown by carbon isotopes in pedogenic carbonates, increasing hematite/goethite values offshore Oman and falling sediment supply rates in the Indus Fan, caused the rainfall maxima to migrate south in the Himalaya. Focused erosion after that time allowed the Inner Lesser Himalaya to duplex and become initially exposed after 9 Ma. Wider exposure was delayed until ~ 6 Ma. Together with unroofing of the Nanga Parbat Massif, this process drove the average ε_{Nd} value of the Indus Delta to more negative values, removing the need for major drainage reorganization to account for this trend. Focused erosion encouraged thrust duplex formation in the Inner Lesser Himalaya, facilitating the exposure both of this unit and the Greater Himalaya after ~ 6 Ma. This explains the relatively late appearance of kyanite and sillimanite in sediments of the Middle and Upper Siwaliks respectively. Climate as well as solid Earth tectonic forces is seen to be crucial in the formation of the NW Himalaya.

Abbreviations

DSDP: Deep Sea Drilling Project; IODP: International Ocean Discovery Program; ITCZ: Intertropical Convergence Zone; MCT: Main Central Thrust; MFT: Main Frontal Thrust; MMCO: Mid-Miocene Climatic Optimum; ODP: Ocean Drilling Program

Acknowledgements

PC gratefully acknowledges the travel grant from Japan Geoscience Union to attend the JpGU-AGU joint meeting 2017 held at Makuhari, Chiba, Japan, and the Charles T. McCord Chair in Petroleum Geology for other research expenses.

Funding

PC was supported by the Charles T. McCord Jr. Chair in Petroleum Geology.

Author's information

PC is the Charles T. McCord Jr. Professor of Petroleum Geology and Dr. Henry V. Howe Distinguished Professor in Geology and Geophysics at Louisiana State University. He has worked on the geological evolution and erosion history of the Western Himalaya for 20 years focusing on the Indus River system. PC works both on and offshore, most recently as co-chief scientist on IODP Expedition 355 in the Arabian Sea. Prior to 2012, he was Kilgour Professor of Geology at the University of Aberdeen, Scotland.

Competing interests

The author declares that he has no competing interests.

Publisher's Note

Received: 21 July 2017 Accepted: 15 November 2017
Published online: 14 December 2017

References

Ahmad T, Harris N, Bickle M, Chapman H, Bunbury J, Prince C (2000) Isotopic constraints on the structural relationships between the Lesser Himalayan series and the high Himalayan crystalline series, Garhwal Himalaya. Geol Soc Am Bull 112(3):467–477

Ali JR, Aitchison JC (2005) Greater India. Earth Sci Rev 72:169–188

Alizai A, Carter A, Clift PD, VanLaningham S, Williams JC, Kumar R (2011) Sediment provenance, reworking and transport processes in the Indus River by U-Pb dating of detrital zircon grains. Glob Planet Chang 76:33–55. doi:10.1016/j.gloplacha.2010.11.008

Armstrong HA, Allen MB (2011) Shifts in the Intertropical Convergence Zone, Himalayan exhumation, and late Cenozoic climate. Geology 39(1):11–14. doi:10.1130/G31005.1

Balsam WL, Deaton BC (1991) Sediment dispersal in the Atlantic Ocean: evaluation by visible light spectra. Rev Aquat Sci 4:411–447

Bera MK, Sarkar A, Chakraborty PP, Loyal RS, Sanyal P (2008) Marine to continental transition in Himalayan foreland. Geol Soc Am Bull. doi:10.1130/B26265.1

Bernet M, Garver JI (2005) Fission-track analysis of detrital zircon. Rev Min Geochem 58:205–238

Bernet M, van der Beek P, Pik R, Huyghe P, Mugnier J-L, Labrin E, Szulc AG (2006) Miocene to recent exhumation of the central Himalaya determined from combined detrital zircon fission-track and U/Pb analysis of Siwalik sediments, western Nepal. Basin Res 18:393–412. doi:10.1111/j.1365-2117.2006.00303

Betzler C, Eberli GP, Kroon D, Wright JD, Swart PK, Nath BN, Alvarez-Zarikian CA, Alonso-García M, Bialik OM, Blättler CL, Guo JA, Haffen S, Horozai S, Inoue M, Jovane L, Lanci L, Laya JC, Mee ALH, Lüdmann T, Nakakuni M, Niino K, Petruny LM, Pratiwi SD, Reijmer JJG, Reolid J, Slagle AL, Sloss CR, Su X, Yao Z,

Young JR (2016) The abrupt onset of the modern South Asian monsoon winds. Sci Rep:29838. doi:10.1038/srep29838
Bignold SA, Treloar PJ, Petford N (2006) Changing sources of magma generation beneath intra-oceanic island arcs: an insight from the juvenile Kohistan island arc, Pakistan Himalaya. Chem Geol 233(1-2):46–74
Bookhagen B, Thiede RC, Strecker MR (2005) Late Quaternary intensified monsoon phases control landscape evolution in the northwest Himalaya. Geology 33(2):149–152. https://doi.org/10.1130/G20982.1
Boos WR, Kuang Z (2010) Dominant control of the South Asian monsoon by orographic insulation versus plateau heating. Nature 463:218–222. doi:10.1038/nature08707
Burbank DW (1992) Causes of recent Himalayan uplift deduced from deposited patterns in the Ganges basin. Nature 357:680–683
Burbank DW, Beck RA, Mulder T (1996) The Himalayan foreland basin. In: Yin A, Harrison TM (eds) The tectonics of Asia. Cambridge University Press, New York, pp 149–188
Burbank DW, Derry LA, France-Lanord C (1993) Reduced Himalayan sediment production 8 Myr ago despite an intensified monsoon. Nature 364:48–50
Calvès G, Clift PD, Inam A (2008) Anomalous subsidence on the rifted volcanic margin of Pakistan: no influence from Deccan plume. Earth Planet Sci Lett 272:231–239
Calvès G, Huuse M, Clift PD, Brusset S (2015) Giant fossil mass wasting off the coast of West India: the Nataraja submarine slide. Earth Planet Sci Lett 432:265–272. doi:10.1016/j.epsl.2015.10.022
Catlos EJ, Harrison TM, Kohn MJ, Grove M, Ryerson FJ, Manning CE, Upreti BN (2001) Geochronologic and thermobarometric constraints on the evolution of the main central thrust, central Nepal Himalaya. J Geophys Res 106(B8): 16,177–116,204
Célérier J, Harrison TM, Beyssac O, Herman F, Dunlap WJ, Webb AAG (2009a) The Kumaun and Garwhal Lesser Himalaya, India: part 2. Thermal and deformation histories. Geol Soc Am Bull 121(9-10):1281–1297. doi:10.1130/B26343.1
Célérier J, Harrison TM, Webb AAG, Yin A (2009b) The Kumaun and Garwhal lesser Himalaya, India: part 1. Structure and stratigraphy. Geol Soc Am Bull 121(9-10): 1262–1280. doi:10.1130/B26344.1
Chirouze F, Huyghe P, Chauvel C, van der Beek P, Bernet M, Mugnier J-L (2015) Stable drainage pattern and variable exhumation in the Western Himalaya since the Middle Miocene. J Geol 123:1–20. doi:10.1086/679305
Clemens SC, Prell WL, Sun Y (2010) Orbital-scale timing and mechanisms driving Late Pleistocene Indo-Asian summer monsoons: reinterpreting cave speleothem $\partial^{18}O$. Paleoceanography 25 (PA4207). doi:10.1029/2010PA001926
Clift P, Gaedicke C, Edwards R, Lee J II, Hildebrand P, Amjad S, White RS, Schlueter H-U (2002a) The stratigraphic evolution of the Indus fan and the history of sedimentation in the Arabian Sea. Mar Geophys Res 23(3): 223–245
Clift PD (2006) Controls on the erosion of Cenozoic Asia and the flux of clastic sediment to the ocean. Earth Planet Sci Lett 241(3-4):571–580
Clift PD, Blusztajn JS (2005) Reorganization of the western Himalayan river system after five million years ago. Nature 438(7070):1001–1003
Clift PD, Giosan L (2014) Sediment fluxes and buffering in the post-glacial Indus Basin. Basin Res 26:369–386. doi:10.1111/bre.12038
Clift PD, Hodges K, Heslop D, Hannigan R, Hoang LV, Calves G (2008) Greater Himalayan exhumation triggered by Early Miocene monsoon intensification. Nat Geosci 1:875–880. doi:10.1038/ngeo351
Clift PD, Lee JI, Hildebrand P, Shimizu N, Layne GD, Blusztajn J, Blum JD, Garzanti E, Khan AA (2002b) Nd and Pb isotope variability in the Indus River system; implications for sediment provenance and crustal heterogeneity in the western Himalaya. Earth Planet Sci Lett 200(1-2):91–106. doi:10.1016/S0012-821X(02)00620-9
Clift PD, Shimizu N, Layne G, Gaedicke C, Schlüter HU, Clark MK, Amjad S (2001) Development of the Indus fan and its significance for the erosional history of the western Himalaya and Karakoram. Geol Soc Am Bull 113:1039–1051
Clift PD, VanLaningham S (2010) A climatic trigger for a major Oligo-Miocene unconformity in the Himalayan foreland basin. Tectonics 29 (TC5014). doi:10.1029/2010TC002711
Clift PD, Wan S, Blusztajn J (2014) Reconstructing chemical weathering, physical erosion and monsoon intensity since 25 Ma in the northern South China Sea: a review of competing proxies. Earth-Sci Rev 130:86–102. doi:10.1016/j.earscirev.2014.01.002
Copeland P, Harrison TM (1990) Episodic rapid uplift in the Himalaya revealed by 40Ar/39Ar analysis of detrital K-feldspar and muscovite, Bengal fan. Geology 18:354–357. doi:10.1130/0091-7613(1990)018
Critelli S, De Rosa R, Platt JP (1990) Sandstone detrital modes in the Makran accretionary wedge, Southwest Pakistan; implications for tectonic setting and long-distance turbidite transportation. Sediment Geol 68:241–260
Curry WB, Ostermann DR, Guptha MVS, Itekkot V (1992) Foraminiferal production and monsoonal upwelling in the Arabian Sea; evidence from sediment traps. In: Summerhayes CP, Prell WL, Emeis KC (eds) Upwelling systems; evolution since the early Miocene, Special publication, vol 64. Geological Society, London, pp 93–106
Deaton BC, Balsam WL (1991) Visible spectroscopy—a rapid method for determining hematite and goethite concentration in geological materials. J Sediment Petrol 61(4):628–632
DeCelles PG, Gehrels GE, Quade J, LaReau B, Spurlin M (2000) Tectonic implications of U-Pb zircon ages of the Himalayan orogenic belt in Nepal. Science 288(5465):497–499. doi:10.1126/science.288.5465.497
DeCelles PG, Gehrels GE, Quade J, Ojha TP (1998a) Eocene-early Miocene foreland basin development and the history of Himalayan thrusting, western and central Nepal. Tectonics 17(5):741–765
DeCelles PG, Gehrels GE, Quade J, Ojha TP, Kapp PA, Upreti BN (1998b) Neogene foreland basin deposits, erosional unroofing, and the kinematic history of the Himalayan fold-thrust belt, western Nepal. Geol Soc Am Bull 110(1):2–21
DeCelles PG, Giles KA (1996) Foreland basin systems. Basin Res 8(2):105–123
DePaolo DJ, Wasserburg GJ (1976) Inferences about magma sources and mantle structure from variations of $^{143}Nd/^{144}Nd$. Geophys Res Lett 3(12):743–746
Dettman DL, Kohn MJ, Quade J, Ryerson FJ, Ojha TP, Hamidullah S (2001) Seasonal stable isotope evidence for a strong Asian monsoon throughout the past 10.7 m.y. Geology 29(1):31–34
Droz L, Bellaiche G (1991) Seismic facies and geologic evolution of the central portion of the Indus fan. In: Weimer P, Link MH (eds) Seismic facies and sedimentary processes of submarine fans and turbidite systems. Springer Verlag, Berlin, pp 383–402
Dunlap WJ, Wysoczanski R (2002) Thermal evidence for Early Cretaceous metamorphism in the Shyok suture zone and age of the Khardung volcanic rocks, Ladakh, India. J Asian Earth Sci 20(5):481–490
Fraser JE, Searle MP, Parrish RR, Noble SR (2001) Chronology of deformation, metamorphism, and magmatism in the southern Karakoram Mountains. Geol Soc Am Bull 113(11):1443–1455
Garzanti E (1993) Sedimentary evolution and drowning of a passive margin shelf (Giumal Group; Zanskar Tethys Himalaya, India): palaeoenvironmental changes during final break-up of Gondwanaland. In: Treloar PJ, Searle MP (eds) Himalayan tectonics, Special publication, vol 74. Geological Society, London, pp 277–298. doi:10.1144/GSL.SP.1993.074.01.20
Garzanti E, Baud A, Mascle G (1987) Sedimentary record of the northward flight of India and its collision with Eurasia (Ladakh Himalaya, India). Geodin Acta 1(4/5):297–312
Garzanti E, Vezzoli G, Ando S, Paparella P, Clift PD (2005) Petrology of Indus River sands; a key to interpret erosion history of the western Himalayan syntaxis. Earth Planet Sci Lett 229(3-4):287–302. doi:10.1016/j.epsl.2004.11.008
Garzione CN, Dettman DL, Quade J, DeCelles PG, Butler RF (2000) High times on the Tibetan Plateau; paleoelevation of the Thakkhola Graben, Nepal. Geology 28(4):339–342
Gébelin A, Mulch A, Teyssier C, Jessup MJ, Law RD, Brunel M (2013) The Miocene elevation of Mount Everest. Geology 41(7):799–802. doi:10.1130/G34331.1
Gehrels GE, Kapp P, DeCelles P, Pullen A, Blakely R, Weislgel A, Ding L, Guynn J, Marin A, McQuarrie N, Yin A (2011) Detrital zircon geochronology of pre-Tertiary strata in the Tibetan-Himalayan orogen. Tectonics 30 (TC5016). doi:10.1029/2011TC002868
Giosan L, Flood RD, Grutzner J, Mudie P (2002) Paleoceanographic signi¢cance of sediment color on western North Atlantic drifts: II. Late Pliocene-Pleistocene sedimentation. Mar Geol 189:43–61
Goldstein SJ, Jacobsen SB (1988) Nd and Sr isotopic systematics of river water suspended material; implications for crustal evolution. Earth Planet Sci Lett 87(3):249–265
Goodbred SL, Kuehl SA (2000) Enormous Ganges-Brahmaputra sediment discharge during strengthened early Holocene monsoon. Geology 28(12): 1083–1086
Gupta AK, Anderson DM, Overpeck JT (2003) Abrupt changes in the Asian southwest monsoon during the Holocene and their links to the North Atlantic Ocean. Nature 421:354–356
Gupta AK, Yuvaraja A, Prakasam M, Clemens SC, Velu A (2015) Evolution of the South Asian monsoon wind system since the late Middle Miocene. Palaeogeogr Palaeoclimatol Palaeoecol 438:160–167. doi:10.1016/j.palaeo.2015.08.006

Harrison TM, Célérier J, Aikman A, Hermann J, Heizler M (2009) Diffusion of 40Ar in muscovite. Geochim Cosmochim Acta 73:1039–1051

Hildebrand PR, Searle MP, Shakirullah, van Heijst HJ (2000) Geological evolution of the Hindu Kush, NW Frontier Pakistan; active margin to continent-continent collision zone. In: Khan MA, Treloar PJ, Searle MP, Jan MQ (eds) Tectonics of the Nanga Parbat syntaxis and the western Himalaya, Special publication, vol 170. Geological Society, London, pp 277–293

Hodges K (2003) Geochronology and thermochronology in orogenic systems. In: Rudnick R (ed) The crust. Elsevier-Science, Amsterdam, pp 263–292

Hodges KV, Silverberg DS (1988) Thermal evolution of the Greater Himalaya, Garhwal, India. Tectonics 7(3):583–600

Hovius N, Stark CP (2006) Landslide-driven erosion and topographic evolution of active mountain belts. In: Evans SG, Mugnozza GS, Strom A, Hermanns RL (eds) Landslides from massive rock slope failure. Springer Netherlands, Dordrecht, pp 573–590. doi:10.1007/978-1-4020-4037-5_30

Hurford AJ (1986) Cooling and uplift patterns in the Lepontine Alps, South Central Switzerland and an age of vertical movement on the Isubric fault line. Contrib Mineral Petrol 92:413–427

Inam A, Clift PD, Giosan L, Tabrez AR, Tahir M, Rabbani MM, Danish M (2007) The geographic, geological and oceanographic setting of the Indus River. In: Gupta A (ed) Large rivers: geomorphology and management. Wiley, Chichester, pp 333–345

Jain AK, Lal N, Sulemani B, Awasthi AK, Singh S, Kumar R, Kumar D (2009) Detrital-zircon fission-track ages from the lower Cenozoic sediments, NW Himalayan foreland basin: clues for exhumation and denudation of the Himalaya during the India-Asia collision. Geol Soc Am Bull 121(3/4):519–535. doi:10.1130/B26304.1

Johnson NM, Stix J, Tauxe L, Cerveny PF, Tahirkheli RAK (1985) Palaeomagnetic chronology, fluvial processes and tectonic implications of the Siwalik deposits near Chinji Village, Pakistan. J Geol 93:27–40

Khan MA, Stern RJ, Gribble RF, Windley BF (1997) Geochemical and isotopic constraints on subduction polarity, magma sources, and palaeogeography of the Kohistan intra-oceanic arc, northern Pakistan Himalaya. J Geol Soc Lond 154:935–946

Kim J, Hyeong K, Jung HS, Moon JW, Kim KH, Lee I (2006) Southward shift of the Intertropical Convergence Zone in the western Pacific during the late Tertiary: evidence from ferromanganese crusts on seamounts west of the Marshall Islands. Paleoceanography 21 (Pa4218). doi: doi:10.1029/2006pa001291

Kolla V, Coumes F (1987) Morphology, internal structure, seismic stratigraphy, and sedimentation of Indus fan. AAPG Bull 71:650–677

Kroon D, Steens T, Troelstra SR (1991) Onset of monsoonal related upwelling in the western Arabian Sea as revealed by planktonic foraminifers. In: Prell W, Niitsuma N (eds) Proceedings of the ocean drilling program, scientific results, vol 117. Ocean Drilling Program, College Station, pp 257–263

Kutzbach JE, Prell WL, Ruddiman WF (1993) Sensitivity of Eurasian climate to surface uplift of the Tibetan Plateau. J Geol 101:177–190

Lee JI, Clift PD, Layne G, Blum J, Khan AA (2003) Sediment flux in the modern Indus River traced by the trace element composition of detrital amphibole grains. Sediment Geol 160:243–257. doi:10.1016/S0037-0738(02)00378-0

Licht A, van Cappelle M, Abels HA, Ladant J-B, Trabucho-Alexandre J, France-Lanord C, Donnadieu Y, Vandenberghe J, Rigaudier T, Lecuyer C, Terry D, Adriaens R, Boura A, Guo Z, Soe AN, Quade J, Dupont-Nivet G, Jaeger J-J (2014) Asian monsoons in a late Eocene greenhouse world. Nature 513:501–506. doi:10.1038/nature13704

Liu F, Li J (2015) Landslide erosion associated with the Wenchuan earthquake in the Minjiang River watershed: implication for landscape evolution of the Longmen Shan, eastern Tibetan Plateau. Nat Hazards 76(3):1911–1926. https://doi.org/10.1007/s11069-014-1575-8

Lyle MW, Wilson PA, Janecek TR, Shipboard party (2002) Leg 199 summary. In: Lyle MW, Wilson P, Janecek TR (eds) Proceedings of the ocean drilling program, initial reports, vol 199. Ocean Drilling Program, College Station, pp 1–89

Malavieille J (2010) Impact of erosion, sedimentation, and structural heritage on the structure and kinematics of orogenic wedges: analog models and case studies. GSA Today 20(1). doi:10.1130/GSATG48A.1

Meigs AJ, Burbank DW, Beck RA (1995) Middle-late Miocene (>10 Ma) formation of the main boundary thrust in the western Himalaya. Geology 23(5):423–426

Miles PR, Roest WR (1993) Earliest seafloor spreading magnetic anomalies in the north Arabian Sea and the ocean-continent transition. Geophys J Int 115:1025–1031

Molnar P, England P, Martinod J (1993) Mantle dynamics, uplift of the Tibetan Plateau, and the Indian monsoon. Rev Geophys 31(4):357–396

Montgomery DR, Stolar DB (2006) Reconsidering Himalayan river anticlines. Geomorphology 82:4–15. doi:10.1016/j.geomorph.2005.08.021

Naini BR, Kolla V (1982) Acoustic character and thickness of sediments of the Indus fan and the continental margin of western India. Mar Geol 47:181–195

Najman Y (2006) The detrital record of orogenesis: a review of approaches and techniques used in the Himalayan sedimentary basins. Earth-Sci Rev 74(1-2):1–72

Najman Y, Bickle M, Garzanti E, Pringle M, Barfod D, Brozovic N, Burbank D, Ando S (2009) Reconstructing the exhumation history of the Lesser Himalaya, NW India, from a multitechnique provenance study of the foreland basin Siwalik Group. Tectonics 28 (TC5018). doi:10.1029/2009TC002506

Najman Y, Garzanti E (2000) Reconstructing early Himalayan tectonic evolution and paleogeography from Tertiary foreland basin sedimentary rocks, northern India. Geol Soc Am Bull 112(3):435–449

Najman Y, Pringle M, Godin L, Oliver G (2001) Dating of the oldest continental sediments from the Himalayan foreland basin. Nature (London) 410(6825): 194–197

Najman YMR, Pringle MS, Johnson MRW, Robertson AHF, Wijbrans JR (1997) Laser 40Ar/39Ar dating of single detrital muscovite grains from early foreland-basin sedimentary deposits in India; implications for early Himalayan evolution. Geology 25(6):535–538

Ojha TP, Butler RF, Quade J, DeCelles PG, Richards D, Upreti BN (2000) Magnetic polarity stratigraphy of the Neogene Siwalik Group at Khutia Khola, far western Nepal. Geol Soc Am Bull 112(3):424–434

Pan F-B, Zhang H-F, Harris N, W-C X, Guo L (2012) Oligocene magmatism in the eastern margin of the east Himalayan syntaxis and its implication for the India-Asia post-collisional process. Lithos 154:181–192. doi:10.1016/j.lithos.2012.07.004

Pandey DK, Clift PD, Kulhanek DK, Expedition 355 Scientists (2015) Arabian Sea Monsoon. Int Ocean Disc Prog Prelim Rpt 355. doi:10.2204/iodp.pr.355.2015

Phillips RJ, Parrish RR, Searle MP (2004) Age constraints on ductile deformation and long-term slip rates along the Karakoram fault zone, Ladakh. Earth Planet Sci Lett 226:305–319

Prell WL, Murray DW, Clemens SC, Anderson DM (1992) Evolution and variability of the Indian Ocean summer monsoon: evidence from the western Arabian Sea drilling program. In: Duncan RA, Rea DK, Kidd RB, von Rad U, Weissel JK (eds) Synthesis of results from scientific drilling in the Indian Ocean, Geophysical monograph, vol 70. American Geophysical Union, Washington, DC, pp 447–469

Quade J, Cerling TE (1995) Expansion of C4 grasses in the late Miocene of northern Pakistan: evidence from stable isotopes in Paleosols. Palaeogeogr Palaeoclimatol Palaeoecol 115(1-4):91–116

Quade J, Cerling TE, Bowman JR (1989) Development of Asian monsoon revealed by marked ecological shift during the latest Miocene in northern Pakistan. Nature 342(6246):163–166

Raiverman V, Kunte SV, Mukherjea A (1983) Basin geometry, Cenozoic sedimentation and hydrocarbon prospects in northwestern Himalaya and Indo–Gangetic plains. Petrol Asia J 6:67–92

Raiverman V, Raman KS (1971) Facies relations in the Subathu sediments, Simla Hills, N.W. Himalaya, India. Geol Mag 108:329–341

Rao AR (1993) Magnetic-polarity stratigraphy of upper Siwalik of north-western Himalayan foothills. Curr Sci 64(11/12):863–873

Replumaz A, Negredo AM, Villaseñor A, Guillot S (2010) Indian continental subduction and slab break-off during tertiary collision. Terra Nova 22:290–296. doi:10.1111/j.1365-3121.2010.00945.x

Robertson AHF, Collins AS (2002) Shyok suture zone, N Pakistan; late Mesozoic-Tertiary evolution of a critical suture separating the oceanic Ladakh Arc from the Asian continental margin. J Asian Earth Sci 20(3):309–351

Robertson AHF, Degnan PJ (1994) The Dras arc complex: lithofacies and reconstruction of a late cretaceous oceanic volcanic arc in the Indus suture zone, Ladakh Himlaya. Sediment Geol 92:117–145

Roddaz M, Said A, Guillot S, Antoine PO, Montel JM, Martin F, Darrozes J (2011) Provenance of Cenozoic sedimentary rocks from the Sulaiman fold and thrust belt, Pakistan: implications for the palaeogeography of the Indus drainage system. J Geol Soc Lond 168:499–516. doi:10.1144/0016-76492010-100

Rowley DB, Currie BS (2006) Palaeo-altimetry of the late Eocene to Miocene Lunpola basin, central Tibet. Nature 439:677–681

Schärer U, Copeland P, Harrison TM, Searle MP (1990) Age, cooling history, and origin of post-collisional leucogranites in the Karakoram Batholith; a multi-system isotope study. J Geol 98(2):233–251

Schwertmann U (1971) Transformation of hematite to goethite in soils. Nature 232:624–625

Searle MP (1996) Cooling history, erosion, exhumation and kinematics of the Himalaya-Karakoram-Tibet orogenic belt. In: Yin A, Harrison TM (eds) The tectonic evolution of Asia. Cambridge University Press, Cambridge, pp 110–137
Searle MP, Fryer BJ (1986) Garnet, tourmaline and muscovite-bearing leucogranites, gneisses and migmatites of the higher Himalayas from Zanskar, Kulu, Lahoul and Kashmir. In: Coward MP, Ries AC (eds), Special Publications, vol 19. Geological Society, London, pp 185-201 doi:10.1144/GSL.SP.1986.019.01.10
Searle MP, Law RD, Jessup M, Simpson RL (2006) Crustal structure and evolution of the greater Himalaya in Nepal – South Tibet: implications for channel flow and ductile extrusion of the middle crust. In: Law RD, Searle MP, Godin L (eds) Channel flow, ductile extrusion and exhumation in continental collision zones, Special publication, vol 268. Geological Society, London, pp 355–378
Searle MP, Rex AJ, Tirrul R, Rex DC, Barnicoat A, Windley BF (1989) Metamorphic, magmatic and tectonic evolution of the central Karakoram in the Biafo-Baltoro-Hushe regions of north Pakistan. Geol Soc Am Spec Pap 232:47–73
Shuaib SM, Tariq Shuaib SM (1999) Geology and oil/Gass presence in the offshore Indus Basin of Pakistan. In: Meadows A, Meadows PS (eds) The Indus River: biodiversity, resources, humankind. Oxford University Press, Karachi, pp 249–265
Simpson G (2004) Role of river incision in enhancing deformation. Geology 32(4): 341–345. https://doi.org/10.1130/G20190.2
Singh S, Parkash B, Awasthi AK, Kumar S (2011) Late Miocene record of palaeovegetation from Siwalik palaeosols of the Ramnagar sub-basin, India. Curr Sci 100(2):213–222
Sinha RN (1970) Heavy mineral investigation of the Siwaliks of Mohand, district Saharanpur, Uttar Pradesh. J Geol Soc India 11:163–177
Stephenson BJ, Searle MP, Waters DJ, Rex DC (2001) Structure of the main central thrust zone and extrusion of the high Himalayan deep crustal wedge, Kishtwar-Zanskar Himalaya. J Geol Soc Lond 158(4):637–652
Szulc AG, Najman Y, Sinclair HD, Pringle M, Bickle M, Chapman H, Garzanti E, Ando S, Huyghe P, Mugnier J-L, Ojha T, DeCelles PG (2006) Tectonic evolution of the Himalaya constrained by detrital 40Ar/39Ar, Sm/Nd and petrographic data from the Siwalik foreland basin succession, SW Nepal. Basin Res 18(4):375–391
Tagami T, Ito H, Nishimura S (1990) Thermal annealing characteristics of spontaneous fi ssion tracks in zircon. Chem Geol 80:159–169
Tauxe L, Opdyke ND (1982) A time framework based on magnetostratigraphy of the Siwalik sediments of the Khaur arae, northern Pakistan. Palaeogeogr Palaeoclimatol Palaeoecol 37:43–61
Treloar PJ, Rex DC, Guise PG, Wheeler J, Hurford AJ, Carter A (2000) Geochronological constraints on the evolution of the Nanga Parbat syntaxis, Pakistan Himalaya. In: Khan MA, Treloar PJ, Searle MP, Jan MQ (eds) Tectonics of the Nanga Parbat syntaxis and the western Himalaya, Geological society special publication, vol 170. Geological Society, London, pp 137–162
Vermeesch P (2012) On the visualisation of detrital age distributions. Chem Geol 312–313:190–194. doi:10.1016/j.chemgeo.2012.04.021
Vidal P, Cocherie A, Le Fort P (1982) Geochemical investigations of the origin of the Manaslu leucogranite (Himalaya, Nepal). Geochim Cosmochim Acta 46: 2279–2292
Walker J, Martin MW, Bowring SA, Searle M, Waters DJ, Hodges K (1999) Metamorphism, melting, and extension: age constraints from the high Himalayan slab of southeast Zanskar and northwest Lahaul. J Geol 107:473–495
Wan S, Clift PD, Li A, Yu Z, Li T, Hu D (2012) Tectonic and climatic controls on long-term silicate weathering in Asia since 5 Ma. Geophys Res Lett 39(L15611). doi:10.1029/2012GL052377
Wan S, Kürschner WM, Clift PD, Li A, Li T (2009) Extreme weathering/erosion during the Miocene climatic optimum: evidence from sediment record in the South China Sea. Geophys Res Lett 36(L19706). doi:10.1029/2009GL040279
Webb AAG (2013) Preliminary palinspastic reconstruction of Cenozoic deformation across the Himachal Himalaya (northwestern India). Geosphere 9:572–587
Webb AAG, Guo H, Clift PD, Husson L, Müller T, Costantino D, Yin A, Xu Z, Cao H, Wang Q (2017) The Himalaya in 3D: slab dynamics controlled mountain building and monsoon intensification. Lithosphere. doi:10.1130/L636.1
West AJ, Galy A, Bickle MJ (2005) Tectonic and climatic controls on silicate weathering. Earth Planet Sci Lett 235:211–228. doi:10.1016/j.epsl.2005.03.020
Whipple KX (2009) The influence of climate on the tectonic evolution of mountain belts. Nat Geosci 2:1–8. doi:10.1038/ngeo413
White NM, Pringle M, Garzanti E, Bickle M, Najman Y, Chapman H, Friend P (2002) Constraints on the exhumation and erosion of the high Himalayan slab, NW India, from foreland basin deposits. Earth Planet Sci Lett 195:29–44
Whitmarsh RB, Weser OE, Ross DA, Shipboard Scientific Party (1974) Site 221. Initial reports of the Deep Sea drilling project, vol 23, pp 167–210
Whittington A, Foster G, Harris N, Vance D, Ayres M (1999) Lithostratigraphic correlations in the western Himalaya—an isotopic approach. Geology 27(7):585–588
Willett SD (1999) Orogeny and orography: the effects of erosion on the structure of mountain belts. J Geophys Res 104:28957–28981
You Y, Huber M, Müller RD, Poulsen CJ, Ribbe J (2009) Simulation of the Middle Miocene climate optimum. Geophys Res Lett 36(4). doi:10.1029/2008GL036571
Zachos J, Pagani M, Sloan L, Thomas E, Billups K (2001) Trends, rythms and abberations in global climate 65 Ma to present. Science 292:686–693
Zeitler PK, Sutter JF, Williams IS, Zartman RE, Tahirkheli RAK (1989) Geochronology and temperature history of the Nanga Parbat-Haramosh Massif, Pakistan. In: Malinconico LL, Lillie RJ (eds) Tectonics of the western Himalayas, Special Paper, vol 232. Geological Society of America, Boulder, pp 1–22
Zhang L-Y, Ducea MN, Ding L, Pullen A, Kapp P, Hoffman D (2014) Southern Tibetan Oligocene-Miocene adakites: a record of Indian slab tearing. Lithos 210-211:209–223. doi:10.1016/j.lithos.2014.09.029
Zhang Q, Willems H, Ding L, Gräfe K-U, Appel E (2012) Initial India-Asia continental collision and Foreland Basin evolution in the Tethyan Himalaya of Tibet: evidence from Stratigraphy and Paleontology. J Geol 120(2):175–189
Zhang YG, Jia J, Balsam WL, Liu L, Chen J (2007) High resolution hematite and goethite records from ODP 1143, South China Sea: co-evolution of monsoonal precipitation and El Niño over the past 600,000 years. Earth Planet Sci Lett 264(1-2):136–150
Zhuang G, Najman Y, Guillot S, Roddaz M, Antoine P-O, Métaise G, Carter A, Marivaux L, Solangig SH (2015) Constraints on the collision and the pre-collision tectonic configuration between India and Asia from detrital geochronology, thermochronology, and geochemistry studies in the lower Indus basin, Pakistan. Earth Planet Sci Lett 432:363–373. doi:10.1016/j.epsl.2015.10.026